Evanescent-wave Johnson noise in small devices

Vickram N. Premakumar, Maxim G. Vavilov, and Robert Joynt

(Dated: May 4, 2017)

In many quantum computer architectures, the qubits are in close proximity to metallic device elements. The fluctuating currents in the metal give rise to noisy electromagnetic fields that leak out into the surrounding region. These fields are known as evanescent-wave Johnson noise. The noise can decohere the qubits. We present the general theory of this effect for charge qubits subject to electric noise and for spin and magnetic qubits subject to magnetic noise. A mapping of the quantum-mechanical problem onto a problem in classical electrodynamics simplifies the calculations. The focus is on relatively simple geometries in which analytical calculations can be done. New results are presented for the local noise spectral density in the vicinity of cylindrical conductors such as small antennae, noise from objects that can be treated as dipoles, and noise correlation functions for several geometries. We summarize the current state of the comparison of theory with experimental results on decoherence times of qubits. Emphasis is placed on qualitative understanding of the basic concepts and phenomena.

1. INTRODUCTION

The prospect of quantum computing has inspired many designs for the manipulation of small coherent quantum systems - qubits. Qubits are often located very near electrodes that contain many mobile charges and spins. The thermal and quantum motion of these charges and spins creates random electromagnetic fields that can decohere the qubits, an effect strenuously to be avoided. This noise is a species of Johnson noise.

J.B. Johnson discovered this noise in 1927 in the course of a research program to improve the performance of amplifiers [1]. H. Nyquist soon explained it theoretically using ingenious applications of equilibrium thermodynamics to thought experiments [2]. When the general relation of fluctuation and dissipation was discovered by H.B. Callen and T.A. Welton in 1951, they regarded their fluctuation-dissipation theorem (FDT) as a "Generalized Nyquist Relation" [3]. The later, more general, theory of linear response of Kubo developed out of the FDT [4]. This is an interesting example of important and general basic science coming from research on very specific technological issues.

The Nyquist formula is

$$\left\langle V^2 \right\rangle_\omega = 2k_B T \; R\left(\omega\right) \tag{1}$$

where

$$\left\langle V^2 \right\rangle_\omega = \int_{-\infty}^{+\infty} dt \; e^{i\omega t} \left\langle V\left(0\right) V\left(t\right) \right\rangle .$$

Here V is the voltage drop between the ends of a resistor with a possibly frequency-dependent resistance R. The angle brackets are an average over the stationary random process that V represents. The rms voltage noise $\sqrt{\left\langle V^2 \right\rangle_\omega}$ is the quantity usually quoted (in units of volts per root Hertz), since it is often practical to measure the drop with a bandpass filter in a frequency range where R is more or less constant. Johnson himself verified that this formula holds independent of the shape, size, or constitution of the resistor. These days, Eq. (1) is recognized as the high-temperature limit of the more general formula

$$\left\langle V^2 \right\rangle_\omega = \hbar\omega \coth\left(\hbar\omega/2k_B T\right) \; R\left(\omega\right) \tag{2}$$

that follows from the quantum-mechanical version of the FDT. For applications to qubits we need a generalization of the Nyquist form of the FDT, which gives the voltage drop between two points in a resistor. In particular, we need a theory that works between any two points irrespective of whether they are on a resistor; we would also like to understand the connection between the Nyquist relation with that other famous kind of thermal electromagnetic field - blackbody radiation. Quantum field theory gives the needed generalization. The main difficulty is to formulate finite-temperature quantum electrodynamics in such a way that the only inputs required are the macroscopic electric and magnetic response functions $\varepsilon\left(\vec{r},\omega\right)$ and $\mu\left(\vec{r},\omega\right)$. The outputs of the theory are the noise spectral densities, which are the field fluctuations at a single spatial point (sufficient to calculate the decoherence of point qubits), and the noise correlation functions which give the fluctuations at spatially separated points (required to calculate the decoherence of extended qubits). We will give precise definitions of these quantities below. The formalism required to do this was constructed in the 1950s by Lifshitz [5] and Rytov [6] and the theory was further developed by Agarwal [7]. These authors built on earlier work of Casimir [8]. An accessible treatment is given by Lifshitz and Pitayevskii [9]. There is a fairly large literature on the application of this formalism to heat transfer and friction in small devices which has been reviewed by Volokitin and Persson [10].

Before proceeding with the development of the formalism, we first give a qualitative picture of how we expect noise to leak out of metallic device elements, taking the lead from a paper of Pendry [11]. Consider a piece of metal surrounded by an insulator. For the sake of argument, let us specify that the metal is hotter than its environment. The Stefan-Boltzmann formula tells us that the total EM power radiated depends only on the surface area and the temperature of the object, not on its conductivity. The radiation is the result of photons thermally generated in the metal leaking out through the surface. The metal has a dielectric function $\varepsilon\left(\omega\right) = 1 + 4\pi i\sigma/\omega$, where the conductivity σ nearly always satisfies $\sigma/\omega \gg 1$ (and this is true for all frequencies considered in this paper). $|\varepsilon|$ is much greater than unity, so the speed of light (to the extent that it can be defined for the highly overdamped modes of the metal) is small relative to the surrounding insulator. This immediately implies that the photon density of states and the equilibrium density depends on σ. This presents a paradox, since the radiated power is independent of σ. This paradox is resolved by the realization that a high photon density of states is always accompanied by a high probability of internal reflection of the photon [12, 13]. The cancellation of these effects gives the universal coefficient of blackbody radiation. However, internal reflection is always accompanied by an evanescent wave (Fig. 1). This in turn implies that there will be strong Johnson noise near a metallic surface for any material having $|\varepsilon| \gg 1$. This is called evanescent-wave Johnson noise (EWJN). This physical picture tells us that the proper treatment of

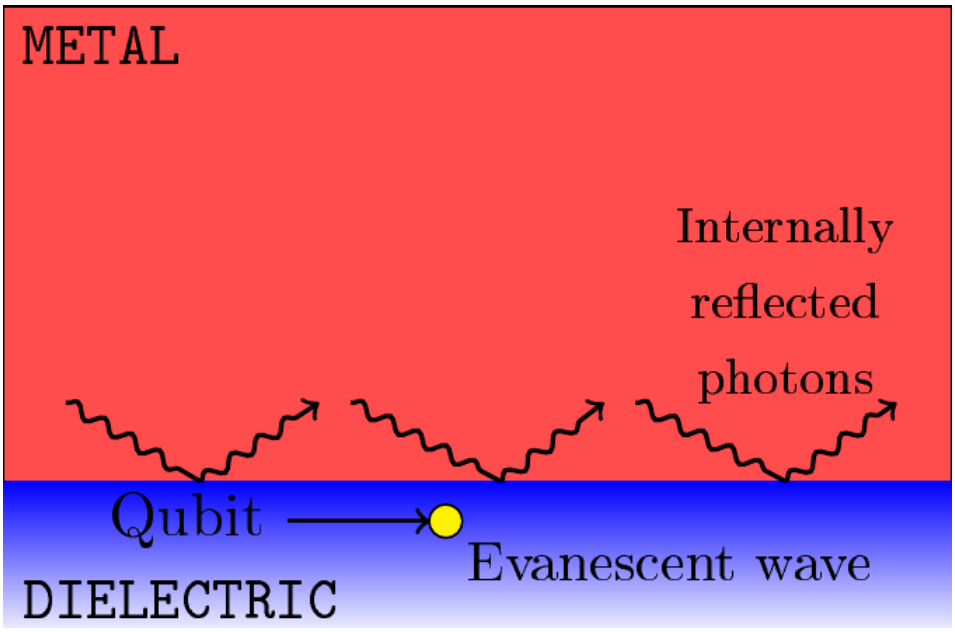

FIG. 1

boundary conditions will be very important. This in turn implies that for ordinary, non-magnetically active metals, the behavior of electric noise is quite different from magnetic noise, since magnetic fields can penetrate those materials much more easily.

It is very important to distinguish between EWJN and the more commonly discussed circuit Johnson noise (CJN). If we consider two separate metallic elements in a small device, usually the path of least resistance between them runs through the external circuit. Thus CJN is a physical effect that involves two or more device elements that convey information about the external circuit to the qubit. EWJN, in contrast, is an effect that occurs even without the external circuit, and fundamentally arises from individual device elements. CJN and EWJN thus come from different physical sources. For the most part, they can be calculated separately and they are basically additive.

The implications of Johnson noise for decoherence of atomic qubits were first discussed by Henkel and collaborators [14, 15] , in the context of heating of trapped ions by the walls of the trap. The local noise spectral densities for both electric and magnetic fields relevant to the situation of point qubits near a conducting half-space were calculated and loss and decoherence rates were extracted. These predictions were quantitatively verified in experiments that measured losses from magneto-optical traps [16]. The lifetimes in the experiments are of order 10 s and the distances from the walls 10 to 100 μm. At about the same time, other qubit applications were discussed by Sidles et al. [17]. In semiconductor and some other solid-state implementations of quantum computing, the distance scales are much less than in the atom experiments and this suggests that the effects of Johnson noise could be appreciable for those systems [18–23]. Indeed, a recent experiment with a diamond film containing NV centers on a silver substrate demonstrated decoherence of qubits due to EWJN in a very direct and quantitative fashion [24].

Charge quantum dot qubits displayed lifetimes in the range of $T_1 \sim 10$ ns, which was shorter than expected based on decoherence mechanisms such as coupling to phonons [25–28]. This spurred theoretical work on CJN for double quantum dots [29], and even though it appears that it cannot be the main mechanism in this instance, the effects are still appreciable.

There has been a small amount of work on the very interesting topic of noise from micromagnets implanted in semiconductors [12, 13]. However, in this paper we shall deal only with non-magnetic materials, so the magnetic permeability $\mu = 1$ everywhere. In this paper, we focus exclusively on EWJN. We cover only analytic calculations and physical considerations. Numerical calculations on realistic devices are not included. To our knowledge, no such calculations exist at present, though the calculations in Ref. [12] represent a start in this direction.

The literature at present only contains analytic results for the half-space, single film [30], and two-film geometries. In the next section we outline the basic formalism of EWJN. Sec. 2 describes how to apply the results to compute lifetimes of qubits. Sec. 3 gives the applications to electric field noise and decoherence of charge qubits. Sec. 4 is a parallel discussion for magnetic field noise and spin qubits. Sec. 5 gives the current situation with regard to comparison of theory and experiment. Sec. 6 gives a summary and describes the implications for future qubit designs.

The overall structure of the paper is meant to reflect the logical development of the subject, with reasonably

complete derivations of the main results. If the reader's main concern is just with new results, then these are to be found as follows.

- We present exact analogies to equivalent problems in classical electromagnetic theory that greatly simplify the calculations in Sec. 2.2.
- We provide explicit results for the noise spectral density that determines the decoherence of point qubits for new geometries. We find that for the conducting cylinder and electrode, the spectral densities exhibit anisotropies. These anisotropies can serve as a sharp criterion for the presence of EWJN. They can also be exploited to substantially increase T_1 and T_2 by suitable qubit orientation. These results are found in Secs. $4.1-4.3$ and $5.1-5.3$.
- We compute noise correlation functions that are needed for the determination of decoherence times for extended qubits. These results are found in Secs. $4.1-4.3$ and $5.1-5.3$.
- We describe in detail how to apply these noise calculations to compute relaxation and decoherence times for qubits in the noise field. These results are found in Sec. 3.1 and 3.2.

Overall, the comparisons with present experimental results indicate that EWJN is not the dominant relaxation mechanism for many charge qubit implementations. On the other hand, the observed relaxation time for certain spin qubits can be explained by the calculations we present here.

2. GENERAL FORMALISM

2.1. Photon Green's Functions

We consider a system at temperature T and regard the dielectric function $\varepsilon(\vec{r},\omega)$ as given. As stated above, $\mu=1$ everywhere so $\vec{B}=\vec{H}$. We will work in the realm of macroscopic electrodynamics, i.e., all quantities are averaged over distances of order a, where a is an interatomic distance. This excludes a large class of physical situations that can be important in qubit devices, namely those in which the noise sources are few in number or otherwise cannot cannot be be considered as members of a continuum. The results in this paper do not apply to such situations.

Our derivation in this section follows Ref. [9]. We present it here to introduce the concepts and to establish notation.

We shall work in the temporal gauge where the scalar potential $\phi=0$. The retarded photon Green's function is

$$iG_{ij}(\vec{r},t;\vec{r}',t')=\Theta(t-t')\left\langle \widehat{A}_i(\vec{r},t)\,\widehat{A}_j(\vec{r}',t')-\widehat{A}_j(\vec{r}',t')\,\widehat{A}_i(\vec{r},t)\right\rangle .$$

Here $\Theta(x)=1$ if $x>0$ and $\Theta(x)=0$ if $x<0$. i,j run over x,y,z. The angle brackets represent a thermal ensemble average. The $\widehat{A}$ are photon operators for the vector potential in the interaction picture. Since for a closed system we have

$$G_{ij}(\vec{r},t;\vec{r}',t')=G_{ij}(\vec{r},\vec{r}',t-t') \tag{3}$$

we define

$$G_{ij}(\vec{r},\vec{r}',\omega)=\int_{-\infty}^{\infty}dt\;e^{i\omega t}G_{ij}(\vec{r},t;\vec{r}',0) \tag{4}$$

and this function satisfies an Onsager relation:

$$G_{ji}(\vec{r}',\vec{r},\omega)=G_{ij}(\vec{r},\vec{r}',\omega). \tag{5}$$

Fortunately, we will not need to consider the operator properties of $\widehat{A}$ in detail. Instead, we will derive a differential equation for G. In the presence of a classical current $\vec{J}$, H' is the perturbation to the free-space Maxwell Hamiltonian with

$$H'=-\frac{1}{c}\int J_i(\vec{r},t)\;\;A_i\;d^3r, \tag{6}$$

with a summation convention over Cartesian indices. The expectation value of $\widehat{A}_i$ is given by the Kubo formula

$$\left\langle \widehat{A}_i\left(\vec{r},\omega\right)\right\rangle = -\frac{1}{\hbar c}\int G_{ij}\left(\vec{r},\vec{r}',\omega\right)\ J_j\left(\vec{r}',\omega\right)\ d^3r'. \tag{7}$$

In the following, angle brackets and the argument ω will often be omitted.

In many situations electronic length scales such as the mean free path ℓ is much smaller than all the other lengths in the problem and consequently there is a local relation between the electric displacement and the electric field: $\vec{D}\left(\vec{r}\right) = \varepsilon\left(\vec{r}\right)\ \vec{E}\left(\vec{r}\right)$. Then Maxwell's equation is

$$\nabla \times \vec{B} = \frac{4\pi}{c}\vec{J} - i\frac{\omega}{c}\varepsilon\left(\vec{r}\right)\vec{E}, \tag{8}$$

and the fields are given in this gauge by

$$\vec{B} = \nabla \times \vec{A} \text{ and } \vec{E} = i\frac{\omega}{c}\vec{A}. \tag{9}$$

Thus we have that

$$-\nabla^2\vec{A} + \nabla\left(\nabla\cdot\vec{A}\right) - \frac{\omega^2\varepsilon\left(\vec{r}\right)}{c^2}\vec{A} = \frac{4\pi}{c}\vec{J} \tag{10}$$

which in index notation with the summation convention is

$$\left[-\delta_{ij}\left(\nabla^2 + \frac{\omega^2\varepsilon\left(\vec{r}\right)}{c^2}\right) + \partial_i\partial_j\right]A_i = \frac{4\pi}{c}J_j. \tag{11}$$

Applying the operator in square brackets to both sides of 7 gives

$$\frac{4\pi}{c}J_j\left(\vec{r}\right) = -\frac{1}{\hbar c}\int\left\{\left[-\delta_{ij}\left(\nabla^2 + \frac{\omega^2\varepsilon\left(\vec{r}\right)}{c^2}\right) + \partial_i\partial_j\right]G_{ik}\left(\vec{r},\vec{r}'\right)\right\}\ J_k\left(\vec{r}'\right)\ d^3r'. \tag{12}$$

Since this is true for any J, it implies that

$$\left[-\delta_{ij}\left(\nabla^2 + \frac{\omega^2\varepsilon\left(\vec{r}\right)}{c^2}\right) + \partial_i\partial_j\right]G_{ik}\left(\vec{r},\vec{r}'\right) = -4\pi\hbar\ \delta^3\left(\vec{r}-\vec{r}'\right)\delta_{jk}. \tag{13}$$

The differential operators act on $\vec{r}$, not $\vec{r}'$. For a fixed $\vec{r}'$ (source position), this is an inhomogeneous partial differential equation when $j = k$ and a homogeneous partial differential equation when $j \neq k$ for the functions G_{jk}. Tangential $\vec{E}$, normal $D = \varepsilon\vec{E}$ and $\vec{B} = \vec{H}$ are continuous at the boundary between different media. We have that $E_i\left(\vec{r}\right) \sim \left(i\omega/c\right)G_{ij}\left(\vec{r},\vec{r}'\right)$ and $B_i\left(\vec{r}\right) \sim \varepsilon_{imn}\partial_m G_{nj}\left(\vec{r},\vec{r}'\right)$. Hence the boundary conditions at a surface with a discontinuity in $\varepsilon\left(\vec{r}\right)$ with normal vector $\widehat{n}$ are:

$$\begin{array}{rl} \epsilon_{ijk}n_i G_{jm} & \text{continuous for all } k,m \\ \varepsilon n_i G_{im} & \text{continuous for all } m \\ \epsilon_{ijk}\partial_i G_{jm} & \text{continuous for all } k,m. \end{array}$$

Now assume that we can solve these differential equations and have the response function G. Then an application of the FD theorem yields

$$\int e^{i\omega\left(t-t'\right)}\left\langle A_i\left(\vec{r},t\right)A_j\left(\vec{r}',t'\right)\right\rangle\ d\left(t-t'\right) \tag{14}$$

$$= \left\langle A_i\left(\vec{r}\right)A_j\left(\vec{r}'\right)\right\rangle_\omega \tag{15}$$

$$= -\coth\left(\frac{\hbar\omega}{2k_BT}\right)\times \operatorname{Im} G_{ij}\left(\vec{r},\vec{r}',\omega\right). \tag{16}$$

As we will see below, the relaxation of a charge qubit with level separation ω in the neighborhood of $\vec{r}$ and $\vec{r}'$ will be determined by a correlation function of the type

$$\left\langle E_i\left(\vec{r}\right)E_j\left(\vec{r}'\right)\right\rangle_\omega = -\frac{\omega^2}{c^2}\coth\left(\frac{\hbar\omega}{2k_BT}\right)\operatorname{Im} G_{ij}\left(\vec{r},\vec{r}',\omega\right). \tag{17}$$

The relaxation of a spin qubit with level separation ω in the neighborhood of $\vec{r}$ and $\vec{r}'$ will be determined by a correlation function of the type

$$\langle B_i(\vec{r})\, B_j(\vec{r}')\rangle_\omega = -\coth\left(\frac{\hbar\omega}{2k_BT}\right) \times \epsilon_{ikm}\epsilon_{jnp}\partial_k\partial'_n \operatorname{Im} G_{mp}(\vec{r},\vec{r}',\omega)\,. \tag{18}$$

We shall also have occasion to refer to the mixed correlation function

$$\langle E_i(\vec{r})\, B_j(\vec{r}')\rangle_\omega = -\frac{i\omega}{c}\coth\left(\frac{\hbar\omega}{2k_BT}\right) \times \epsilon_{jkl}\partial'_k \operatorname{Im} G_{il}(\omega,r,r'). \tag{19}$$

2.2. Physical Analogy

Physical intuition for the meaning of $G_{ik}(\vec{r},\vec{r}',\omega)$, and a practical calculation method, may be obtained by noting the similarity of Eqs. 11 and 13. Place a fictitious point electric dipole $\vec{p}$ at the point $\vec{r}'$. The current is

$$\vec{J}^{(f)}(\vec{r}) = -i\omega\vec{p}\,\delta^3(\vec{r}-\vec{r}')\,.$$

and the resulting fictitious vector potential and the electric field are given by

$$\left[\partial_i\partial_l - \delta_{il}\nabla^2 - \delta_{il}\,\frac{\omega^2\varepsilon(\vec{r})}{c^2}\right] A_l^{(f)}(\vec{r}) = -i\omega p_i\frac{4\pi}{c}\delta^3(\vec{r}-\vec{r}')$$

and

$$\left[\partial_i\partial_l - \delta_{il}\nabla^2 - \delta_{il}\,\frac{\omega^2\varepsilon(\vec{r})}{c^2}\right] E_l^{(f)}(\vec{r}) = p_i\frac{4\pi\omega^2}{c^2}\delta^3(\vec{r}-\vec{r}')\,. \tag{20}$$

On the other hand, multiplying Eq. (13) by p_k and summing over k we find:

$$\left[\partial_i\partial_l - \delta_{il}\nabla^2 - \delta_{il}\,\frac{\omega^2\varepsilon(\vec{r})}{c^2}\right] G_{lk}(\omega;\vec{r},\vec{r}')\,p_k = -4\pi\hbar\; p_i\;\delta^3(\vec{r}-\vec{r}')\,. \tag{21}$$

Comparison of Eqs. (20) and (21) says that

$$G_{lk}(\omega;\vec{r},\vec{r}')\,p_k = -\frac{\hbar c^2}{\omega^2}E_l^{(f)}. \tag{22}$$

and, using Eq. (17)

$$\langle E_i(\vec{r})\, E_j(\vec{r}')\rangle_\omega\;\; p_j = \hbar\coth\left(\frac{\hbar\omega}{2k_BT}\right)\operatorname{Im} E_i^{(f)}\;\text{(no sum)}. \tag{23}$$

Hence if we wish to find (say) G_{xy}, we solve the fictitious classical problem of an oscillating dipole $\vec{p}=(0,p_y,0)$ at the point $\vec{r}'$ and compute $E_x^{(f)}$ at the point $\vec{r}$. Then

$$G_{xy}(\vec{r},\vec{r}') = -\frac{\hbar c^2}{\omega^2}E_x^{(f)}/p_y. \tag{24}$$

We can compute all 9 components of G in this way. There is a similar analogy for magnetic fluctuations. The current of a point magnetic dipole $\vec{m}$ at $\vec{r}'$ may be written as

$$J_i^{(f)}(\vec{r}) = c\;\varepsilon_{ijk}\;\partial_j\delta^3(\vec{r}-\vec{r}')\;\; m_k.$$

The equation for the vector potential in this situation is

$$\left[\partial_i\partial_l - \delta_{il}\nabla^2 - \delta_{il}\ \frac{\omega^2\varepsilon\left(\vec{r}\right)}{c^2}\right]\ A_l^{(f)}\left(\vec{r}\right) \tag{25}$$

$$= -4\pi\ \varepsilon_{ijk}\ \partial_j'\delta^3\left(\vec{r}-\vec{r}'\right)\ m_k. \tag{26}$$

Multiplying Eq. (13) by $\epsilon_{kmn}\ \partial_m' m_n/\hbar$ and summing over m and n we find

$$\left[-\delta_{ij}\left(\nabla^2 + \frac{\omega^2\varepsilon\left(\vec{r}\right)}{c^2}\right) + \partial_i\partial_j\right]\frac{1}{\hbar}\epsilon_{kmn}\ m_n\partial_m' G_{ik}\left(\vec{r},\vec{r}'\right)$$

$$= -4\pi\epsilon_{jmn}\ \partial_m' m_n\delta^3\left(\vec{r}-\vec{r}'\right). \tag{27}$$

Equating the curl of Eqs. (26) and (27) yields

$$\frac{1}{\hbar}\epsilon_{ijk}\epsilon_{lmn}\ m_n\partial_i\partial_m' G_{jl}\left(\vec{r},\vec{r}'\right) = B_k^{(f)}\left(\vec{r},\vec{r}'\right). \tag{28}$$

Hence if we wish to find the magnetic correlations, we first solve the fictitious classical problem of the magnetic field $\vec{B}^{(f)}(\vec{r},\vec{r}')$ at the point $\vec{r}$ resulting from an oscillating point magnetic dipole $\vec{m}$ at the point $\vec{r}'$. For example, to find the physical magnetic field noise spectral density we place a point magnetic dipole $\vec{m}$ in the jth direction at $\vec{r}'$, compute $B_i^{(f)}\left(\vec{r},\vec{r}'\right)$, and then

$$\left\langle B_i\left(\vec{r}\right)B_j\left(\vec{r}'\right)\right\rangle = \frac{\hbar}{m_j}\coth(\hbar\omega/2k_BT)\,\mathrm{Im}\,B_i^{(f)}\left(\vec{r},\vec{r}'\right). \tag{29}$$

The Maxwell equations relate $\vec{E}$ at even orders in ω with $\vec{B}$ at odd orders and vice versa, so the theory has two uncoupled sectors. This is the reason that we need the two separate analogies represented by Eqs. (22) and (28).

In the fictitious problem, the equations satisfied by the fields in the vacuum are

$$\nabla^2\vec{E}^{(f)} = 0$$
$$\nabla^2\vec{B}^{(f)} = 0$$
$$\nabla\cdot\vec{E}^{(f)} = 4\pi\rho/\varepsilon_d$$
$$\nabla\cdot\vec{B}^{(f)} = 4\pi\vec{J}/c$$

and in the metal we have

$$\nabla^2\vec{E}^{(f)} + 2i\delta^{-2}\vec{E}^{(f)} = 0$$
$$\nabla^2\vec{B}^{(f)} + 2i\delta^{-2}\vec{B}^{(f)} = 0$$
$$\nabla\cdot\vec{E}^{(f)} = 0$$
$$\nabla\cdot\vec{B}^{(f)} = 4\pi\vec{J}/c,$$

in the quasistatic case. The boundary conditions are that the tangential component of $\vec{E}^{(f)}$ and $\vec{B}^{(f)}$ are continuous at the interface of dielectric and metal, while the normal component $E_n^{(f)}$of $\vec{E}^{(f)}$ satisfies $(4\pi i\sigma/\omega)\,E_n^{(f)}(m) = \varepsilon_d E_n^{(f)}(d)$, where $E_n^{(f)}(m), E_n^{(f)}(d)$ is the normal component of E in the metal (respectively, the dielectric) as the surface is approached. σ is the DC conductivity of the metal. ε_d is the dielectric constant in the dielectric material.

2.3. Quasistatic Approximation

The subject of this paper is the random electric and magnetic fields that decohere qubits in the neighborhood of small metallic objects. The characteristic frequencies for the decoherence rarely exceed a few GHz, so we restrict our attention to frequencies at or below this range. For this reason we employ the quasistatic approximation from the start, setting the vacuum wavevector $k = \omega/c = 0$. In the interior of a metal object with conductivity σ the characteristic length scale of the fields is the skin depth $\delta = c/\sqrt{2\pi\sigma\omega}$. The inverse skin depth $\delta^{-1} = c/\sqrt{2\pi\sigma\omega}$ is proportional to $\sqrt{(\sigma/\omega)}k \gg k$ and it is retained in the theory. For example, the term $\omega^2\varepsilon\left(\vec{r}\right)/c^2$ in Eq. (11) can be neglected when $\vec{r}$ is in the dielectric or vacuum where $\varepsilon \sim 1$ but not when $\vec{r}$ is in the metal. In this approximation, radiation fields are neglected. We assume that the Drude model is a good approximation for the metals in question, and that $\omega \ll 1/\tau$, where τ is the relaxation time of electrons in the metals. The dielectric function is always approximated as $\varepsilon = 4\pi i\sigma/\omega$.

2.4. Nonlocal Effects

This paper focuses on the cases where local response is valid. Roughly speaking, this is when the distance of $\vec{r}$ and $\vec{r}'$ from the nearest metal surface is greater than the electron mean free path in the metal. However, when the distance to the metal tends to zero, the local expressions for noise strengths diverge, which is clearly unphysical. For completeness, we briefly outline how to include nonlocality in the theory. Generally $\vec{D}(\vec{r})$, the electric displacement, depends on $\vec{E}(\vec{r}')$ according to $D_i(\vec{r},t) = \int d^3r'\ \varepsilon_{ij}(\vec{r}-\vec{r}', t-t')\, E_j(\vec{r}', t')$ and when Fourier transformed this becomes $D_i\left(\vec{k},\omega\right) = \varepsilon_{ij}\left(\vec{k},\omega\right) E_j\left(\vec{k},\omega\right)$. Eq. (13) becomes

$$\left(-\delta_{ij}\nabla^2 + \partial_i\partial_j\right) G_{ik}(\vec{r},\vec{r}') - \delta_{ij}\frac{\omega^2}{c^2}\int d^3r''\varepsilon_{im}(\vec{r},\vec{r}'')\, G_{mk}(\vec{r}'',\vec{r}') \tag{30}$$

$$= -4\pi\hbar\delta^3(\vec{r}-\vec{r}')\,\delta_{jk}. \tag{31}$$

Use of this equation with an appropriate choice for $\varepsilon(\vec{r},\vec{r}'')$ cures the unphysical divergence at small distances. In practice, to date only the problems of a conducting half-space and conducting films have been treated using the nonlocal formalism [22, 23, 30].

3. APPLICATION TO QUBITS

3.1. Relaxation

A qubit system in a noisy environment is described by a Hamiltonian $H = H_q + H_n(t)$ where H_q admits two eigenstates $|0\rangle, |1\rangle$ such that $H_q|i\rangle = \epsilon_i|i\rangle$. The relaxation rate for such a qubit in the presence of EWJN is given by the Golden Rule-type formula

$$\frac{1}{T_1} = \frac{1}{\hbar^2}\int_{-\infty}^{\infty} \overline{\langle 0|H_n(t)|1\rangle\langle 1|H_n(0)|0\rangle} e^{-i\omega t}dt \tag{32}$$

Consider a qubit with charge, mass, and g-factor e, m, and g respectively placed in a time dependent electromagnetic field described by $\vec{A}(r,t)$. The full Hamiltonian is

$$H = \frac{1}{2m}\left(\vec{\Pi} - \frac{e}{c}\vec{A}\right)^2 + V(\vec{r}) - \frac{eg}{2m}\vec{B}\cdot\vec{S},$$

where $\vec{\Pi} = -i\hbar\nabla$. Here we will restrict ourselves to $\mathcal{O}(e)$ so the Hamiltonian can be written

$$H = \frac{\vec{\Pi}^2}{2m} + V(\vec{r}) - \frac{e}{2mc}\left(\vec{\Pi}\cdot\vec{A} + \vec{A}\cdot\vec{\Pi}\right) - \frac{eg}{2m}\vec{B}\cdot\vec{S}. \tag{33}$$

Imposing the gauge condition $\phi = 0$ we find a Hamiltonian readily treated in the interaction picture. The charge distribution generating the noise is contained in the metal, so at a nearby qubit we have $\nabla\cdot E = \nabla^2\phi + \frac{1}{c}\partial_t(\nabla\cdot\vec{A}) = 0$. For finite frequency noise, this implies $\nabla\cdot\vec{A} = 0$, and thus $[\vec{\Pi}, \vec{A}(\vec{r})] = -i\hbar\nabla\cdot\vec{A}(\vec{r}) = 0$. The time dependence of the system is entirely due to the electromagnetic noise and the static Hamiltonian $H_q = \frac{\vec{\Pi}^2}{2m} + V(\vec{r})$. We are left with

$$H = H_q + H_n(t)$$

$$H_n(t) = -\frac{e}{mc}\vec{A}(r,t)\cdot\vec{\Pi} - \frac{eg}{2mc}\vec{B}(r,t)\cdot\vec{S}. \tag{34}$$

Our interaction Hamiltonian can be written as a spatial Taylor series as follows

$$H_n(t) = -\frac{e}{mc}\left[A_i(0,t) + \left(\nabla_j A_i(r,t)\right)_{r=0} r_j + \dots\right]\Pi_i - \frac{eg}{2mc}B_iS_i.$$

This allows us to treat the relevant matrix elements term by term in multipole moments, as described in [31]. Truncating the series at second order and evaluating the off-diagonal matrix elements gives us

$$\frac{1}{T_1^E} = \frac{1}{\hbar^2}\left\langle p_i\right\rangle \left\langle p_l\right\rangle^* \left\langle E_i E_l\right\rangle_\omega \quad ; \quad \frac{1}{T_1^B} = \frac{1}{\hbar^2}\left\langle m_i\right\rangle \left\langle m_l\right\rangle^* \left\langle B_i B_l\right\rangle_\omega \tag{35}$$

$$\frac{1}{T_1^{cross}} = \frac{1}{\hbar^2}\left(\left\langle p_i\right\rangle \left\langle m_n\right\rangle^* \left\langle E_i B_n\right\rangle_\omega + \left\langle m_k\right\rangle \left\langle p_l\right\rangle^* \left\langle B_k E_l\right\rangle_\omega\right).$$

Above we set $\hbar\omega = \epsilon_1 - \epsilon_0$ via Eq. (32). For brevity we also use $\langle x\rangle \equiv \langle 0|x|1\rangle$ and $\left\langle F_i(t)F_j(0)\right\rangle_\omega = \left\langle F_i F_j\right\rangle_\omega$. Here we only include dipole contributions; higher order multipole moments and more details of the calculation are treated in the appendix.

In the case of the spin qubit the states $|0\rangle, |1\rangle$ are up and down states of the spin part of the wavefunction. Hence $|0\rangle = |\psi_0\rangle \otimes |\uparrow\rangle$ where $|\psi_0\rangle$ is the orbital part of the wavefunction which is common to both states of the spin qubit. Immediately we see that all the spatial operator matrix elements $\langle p_i\rangle = \langle q_{ij}\rangle = \langle l_i\rangle = 0$. Hence the above expression simplifies to

$$\frac{1}{T_1} = \frac{1}{\hbar^2}\left(\frac{eg}{2m}\right)^2 \left\langle S_k\right\rangle \left\langle S_n\right\rangle^* \left\langle B_k B_n\right\rangle_\omega. \tag{36}$$

For concreteness, suppose the spin qubit is localized in space and arranged so the up and down states are eigenstates of S_z, then we can explicitly compute the matrix elements to find

$$\frac{1}{T_1} = \left(\frac{eg}{4m}\right)^2 \left(\left\langle B_x B_x\right\rangle_\omega + \left\langle B_y B_y\right\rangle_\omega\right). \tag{37}$$

3.2. Dephasing

Qubit relaxation is due to the off-diagonal matrix elements $\langle 0|\, H_n\, |1\rangle$ and $\langle 1|\, H_n\, |0\rangle$ of the noise Hamiltonian. The diagonal elements $\langle 0|\, H_n\, |0\rangle$ and $\langle 1|\, H_n\, |1\rangle$ produce dephasing. If the initial state is $\left(1/\sqrt{2}\right)\left[|0\rangle + |1\rangle\right]$, and the state at time t is $\left(1/\sqrt{2}\right)\left[|0\rangle + e^{i\phi(t)}\,|1\rangle\right]$ then ϕ is random after a time T_2. The basic formulas for T_2 are as follows. We have

$$\frac{1}{T_2} = \frac{1}{2T_1} + \frac{1}{T_\phi}.$$

where T_ϕ is the dephasing time. For a Johnson-type noise mechanism, the Gaussian approximation for T_ϕ should be very accurate, since many modes of the metal contribute to the noise. T_ϕ is then calculated in the following way. Again let the applied field be in the ith direction. The initial condition is $\phi\,(t=0) = 1$. We then repeatedly measure $X = |0\rangle\langle 0| + |1\rangle\langle 1|$, average to get $\overline{X\,(t)}$ and the function $\Gamma_i\,(t)$ is defined by

$$\overline{X\,(t)} = \exp\left[-\Gamma\,(t)\right] X\,(0)\cos\omega t.$$

and the Gaussian result for $\Gamma\,(t)$ is

$$\Gamma\,(t) = \frac{t^2}{2}\int_{-\infty}^{\infty} d\omega\; S\,(\omega)\,\frac{\sin^2\left(\omega t/2\right)}{\left(\omega t/2\right)^2}, \tag{38}$$

with

$$\begin{aligned} S\,(\omega) = \frac{1}{\hbar^2}\int_{-\infty}^{\infty} dt\; \overline{\left[\langle 1|\, H_n\,(t)\,|1\rangle - \;\langle 0|\, H_n\,(t)\,|0\rangle\right]} \\ \times\, \overline{\left[\langle 1|\, H_n\,(0)\,|1\rangle - \;\langle 0|\, H_n\,(0)\,|0\rangle\right]}\; e^{-i\omega t}. \end{aligned} \tag{39}$$

Evidently we need the diagonal matrix elements of the time-dependent part of the Hamiltonian from Eq. (34). Defining moments $p_i = e r_i$ and $m_i = \frac{e}{2mc}(l_i + g S_i)$.

$$\begin{aligned} \langle 1|H_n(t)|1\rangle - \langle 0|H_n(t)|0\rangle = &- B_k(t)\left(\langle m_k\rangle_1 - \langle m_k\rangle_0\right) \\ &+ E_k(t)\left(\langle p_k\rangle_1 - \langle p_k\rangle_0\right) \end{aligned}$$

To keep things short let $\Delta x = (\langle 1|x|1\rangle - \langle 0|x|0\rangle)$ for any operator x. The integral kernel becomes

$$S(\omega) = \frac{1}{\hbar^2}\left[\langle B_i B_j\rangle_\omega \Delta m_i \Delta m_j - \langle B_i E_j\rangle_\omega \Delta m_i \Delta p_j \right. \\ \left. - \langle E_i B_j\rangle_\omega \Delta p_i \Delta m_j + \langle E_i E_j\rangle_\omega \Delta p_i \Delta p_j\right]. \quad (40)$$

In order to make use of Eq. (38) we need to make some mild assumptions on the frequency dependence of the noise spectral density terms. We can write

$$\Gamma(t) = t^2 \int_0^{1/\tau} d\omega \; f(\omega) \; \omega \coth\left(\frac{\hbar\omega}{2k_B T}\right) \frac{\sin^2(\omega t/2)}{(\omega t/2)^2}.$$

Again, $f(\omega)$ contains all the information about conductivity, qubit position, device geometry, etc., but it depends weakly on frequency at low frequency, and here we will take it to be independent of frequency $f(\omega) = f_0$ until it falls rapidly to zero at $\omega = 1/\tau$, where τ is the electron relaxation time. We note first that at very short times ($t \ll \tau, \hbar/k_B T$) we always get $\Gamma(t) \sim t^2/t_0^2$ (Gaussian decay), where

$$t_0^2 = \frac{4\tau^2}{f_0} \tanh\left(\frac{\hbar}{2k_B T\tau}\right).$$

As a result, Gaussian decay is only observed when the noise is quasi-static. Exponential decay at longer times is the most important from the standpoint of EWJN. This is where $t \gg \tau$ and $t \gg \hbar/k_B T$ and then we can write

$$\Gamma(t) = 4f_0 \int_0^{t/2\tau} dx \; \coth\left(\frac{\hbar x}{k_B T t}\right) \frac{\sin^2 x}{x} \\ \approx 2\pi f_0 \; \frac{k_B T t}{\hbar}.$$

Hence, at any experimentally accessible temperature

$$\frac{1}{T_\phi} = \frac{2\pi f_0 k_B T}{\hbar}. \quad (41)$$

We see that only off diagonal elements of the multipole moments determine T_1 and all of the matrix elements come into the determination of T_2. If the expectation values of the multipole moments are not significantly different between the ground and excited qubit states T_ϕ^{-1} will be small and ${T_2}^{-1} \approx (2T_1)^{-1}$. Even if not, T_1 and T_2 will generally be of the same order of magnitude, which distinguishes EWJN from many other noise mechanisms.

In many experiments, it appears that the noise spectrum has two components, a "$1/f$" component that dominates at low frequencies, and a white component that is bigger at high frequencies. Using the qubit as a spectrometer [32] it has been shown that this happens both in GaAs devices [33] and in Si devices [34]. Echo techniques can mitigate the low-frequency noise but not the more pernicious white part. T_2^{echo} , the decoherence time after echoing, can serve as a diagnostic for EWJN in this situation. The experiment of Ref. [33] is particularly interesting in this regard, since it shows that the white component of the noise has a strong temperature dependence which the $1/f$ part is largely temperature (T) independent, strongly suggesting different origins for the two types of noise. However, T_2^{echo} was proportional to T^{-2} , while Eq. (41) would predict a T^{-1} behavior.

4. ELECTRIC NOISE

The noise spectral density $\langle E_i(\vec{r})\, E_j(\vec{r}')\rangle_\omega$ generally involves four length scales: $|\vec{r} - \vec{r}'|$, the distance over which the correlations are to be measured; d, the distance from the qubit to the conducting object(s); $\delta = c/\sqrt{2\pi\sigma\omega}$, the skin depth in the conductor(s); and L, the linear size of the conducting object(s). In most cases, the size of the qubit is small, which means that usually the case $\vec{r} \approx \vec{r}'$ is of interest, and $|\vec{r} - \vec{r}'|$ is the smallest length in the problem. However, qubits can also be extended objects, so we will give formulas as a function of $\vec{r} - \vec{r}'$ where possible. As stated above, the vacuum wavelength is always taken to be infinite. The simple geometries treated in this paper are shown in Fig. 3.

We will focus first on some limiting cases in which at least one of the other three lengths is very different from the two others.

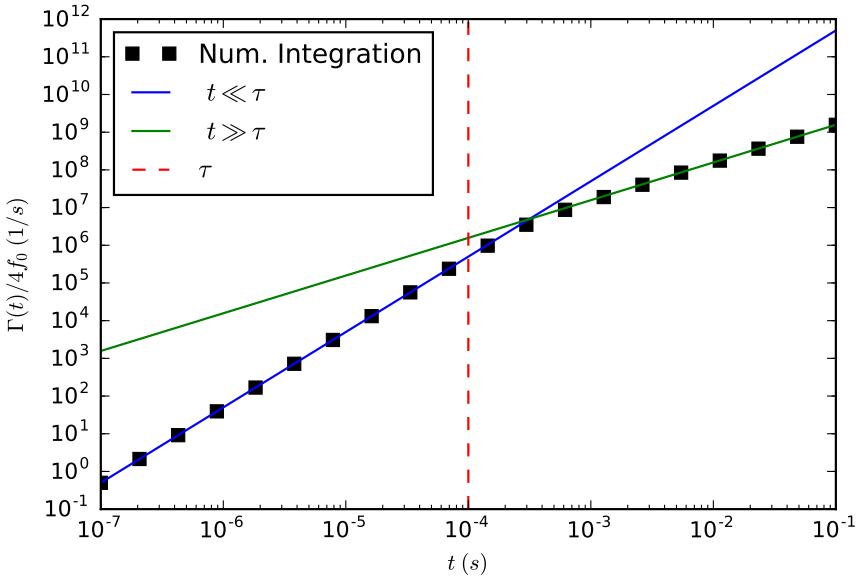

FIG. 2: Eq. (38) for $S(\omega) = f_0\,\omega \coth\left(\frac{\hbar\omega}{2k_BT}\right)$ at $T = 0.1$ K and $\tau = 0.1$ ms plotted alongside approximate results for Gaussian noise ($t \ll \tau$) and exponential decay ($t \gg \tau$).

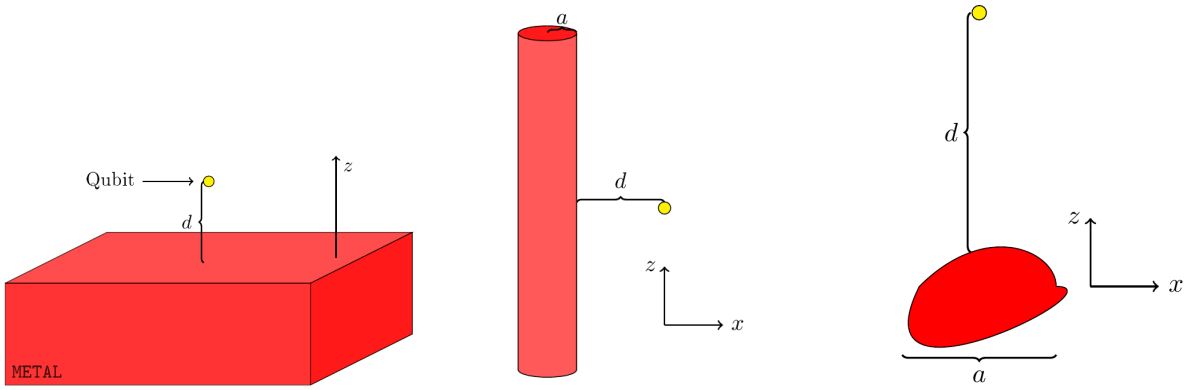

(a) Half Space (b) Cylinder (c) Distant Object

FIG. 3: Various qubit system geometries treated in this paper

4.1. Half Space

4.1.1. Point Qubit

We first focus on some simple methods to compute $G_{ij}\left(\vec{r},\vec{r}'=\vec{r}\right) = \delta_{ij}G_{ii}\left(\vec{r},\vec{r}'=\vec{r}\right)$, which is sufficient for the calculation of the decoherence of a point qubit. This case lends itself to some simple approximations that are physically illuminating

a. Image Regime To understand this problem physically, we first outline the solution when $d \ll \delta$, since the problem is then essentially elementary. The greater part of the electric field is concentrated within a sphere of radius of order d of the dipole. This implies that inside the metal we have that $\nabla^2\vec{E} = \left(-2i/\delta^2\right)\vec{E} \approx 0$, since the skin depth δ may be taken to be large. The problem now reduces to the image problem for a static point charge in a medium with dielectric constant ε_d located at a distance d from a half space with dielectric constant $\varepsilon_m \approx 4\pi i\sigma/\omega$. For $z > 0$ we have the equations $\nabla\cdot\vec{E} = 4\pi\rho = 4\pi\delta^3\left(\vec{r}-\vec{r}'\right)$ and $\nabla\times\vec{E} = 0$. For $z < 0$, we have $\nabla\cdot\vec{E} = 0$ and $\nabla\times\vec{E} = 0$. At the interface we have $\varepsilon_d E_z\left(z = 0_+\right) = \varepsilon_m E_z\left(z = 0_-\right)$ and $E_{x,y}\left(z = 0_+\right) = E_{x,y}\left(z = 0_-\right)$. This is the textbook

image problem. Hence the solution for $z > 0$ is given by $E = -\nabla\Phi$, with $\Phi_1(\vec{r}) = q/|\vec{r} - \vec{r}'| + q'/|\vec{r} - \vec{r}''|$ and for $z < 0$ by $\Phi_2(\vec{r}) = q''/|\vec{r} - \vec{r}'|$. Here $q' = -q[(\varepsilon_m - \varepsilon_d)/(\varepsilon_m + \varepsilon_d)]$ and $q'' = q[(2\varepsilon_m)/(\varepsilon_m + \varepsilon_d)]$. This satisfies the differential equations and the boundary conditions. Hence the textbook image solution carries over to this case.

We will do the $\langle E_x(\vec{r}) E_x(\vec{r})\rangle_\omega$ correlation function first, so we place a fictitious dipole $\vec{p} = p\hat{x}$ at $\vec{r}' = (0, 0, d)$. Then we need the induced field at $\vec{r}$. It is produced by the image dipole $\vec{p}'$ at $\vec{r}''$:

$$p' = -p\frac{\varepsilon_m - \varepsilon_d}{\varepsilon_m + \varepsilon_d} \approx -p\left(1 + \frac{i\omega\varepsilon_d}{2\pi\sigma}\right)$$

and the field from this charge is

$$\begin{aligned} E_x'^{(f)}(\vec{r}) &= p'\frac{3(\vec{r} - \vec{r}'')_x(\vec{r} - \vec{r}'')_x - |\vec{r} - \vec{r}''|^2}{|\vec{r} - \vec{r}''|^5} \\ &= p\left(1 + \frac{i\omega\varepsilon_d}{2\pi\sigma}\right)\frac{1}{(2d)^3} \end{aligned}$$

so

$$G_{xx}(\vec{r}, \vec{r}, \omega) = -\frac{\hbar c^2}{\omega^2}\left(1 + \frac{i\omega\varepsilon_d}{2\pi\sigma}\right)\frac{1}{(2d)^3}$$

and using Eq. (22) we find at the position $\vec{r} = \vec{r}'$ of the qubit that the physical local noise spectral density is

$$\langle E_x(\vec{r}) E_x(\vec{r})\rangle_\omega = \hbar\frac{\omega\varepsilon_d}{16\pi\sigma d^3}\coth\left(\frac{\hbar\omega}{2k_BT}\right). \tag{42}$$

which at low temperatures $k_BT \ll \hbar\omega$ reduces to

$$\langle E_x(\vec{r}) E_x(\vec{r})\rangle_\omega = \hbar\frac{\omega\varepsilon_d}{16\pi\sigma d^3},$$

and at high temperatures $k_BT \gg \hbar\omega$ to

$$\langle E_x(\vec{r}) E_x(\vec{r})\rangle_\omega = \frac{k_BT\varepsilon_d}{8\pi\sigma d^3}.$$

Of course cylindrical symmetry implies that $\langle E_y(\vec{r}) E_y(\vec{r})\rangle_\omega = \langle E_x(\vec{r}) E_x(\vec{r})\rangle_\omega$.

It is important to note that the electric noise is *inversely* proportional to σ. For really good metals, the screening is complete and there is no dissipation and therefore no fluctuations in the field. It is a general result that the result for $\vec{E}^{(f)}$ depends only on the *ratio* of dielectric constants in the two media, that is, on $(4\pi i\sigma/\omega)/\varepsilon_d$. This follows immediately from inspection of the boundary condition, which is the only place that ε_d enters the calculation. The d^{-3} dependence follows immediately from the physical analogy to the image problem.

Now we will do the $\langle E_z(\vec{r}) E_z(\vec{r}')\rangle_\omega$ correlation function, so we place a dipole $\vec{p} = p\hat{z}$ at $\vec{r}' = (0, 0, d)$. Then we need the induced field at $\vec{r}$. The calculation proceeds as for the x direction except for a change in sign of the fictitious image dipole $\vec{p}'$ at $\vec{r}'' = (0, 0, -d)$:

$$p' = p\frac{\varepsilon_m - \varepsilon_d}{\varepsilon_m + \varepsilon_d}$$

with the result that

$$\langle E_z(\vec{r}') E_z(\vec{r}')\rangle_\omega = \hbar\frac{\omega\varepsilon_d}{8\pi\sigma d^3}\coth\left(\frac{\hbar\omega}{2k_BT}\right), \tag{43}$$

which is greater than $\langle E_x(\vec{r}') E_x(\vec{r}')\rangle_\omega$ by a factor of 2. This anisotropy is quite significant for detailed exploration of the theory by experiment.

b. Induction regime This regime is characterized by the opposite limit $d \gg \delta$. The qubit is far away from the interface on the length scale of the penetration depth. The image problem does not carry over directly since the electric field in the metal satisfies $\nabla^2 \vec{E}^{(f)} = \left(-2i/\delta^2\right) \vec{E}^{(f)}$ in the metal and δ^{-2} cannot be neglected, as it was in the image regime. However, we may now use the fact that the field penetrates only a short distance into the metal, and this allows us to develop a perturbation series in ω for the complex amplitudes $\vec{E}^{(f)}, \vec{B}^{(f)}$ in the frequency domain. At order ω^0 we have an electric field $\vec{E}^{(f)}$ but $\vec{B}^{(f)}$ vanishes. $\vec{E}^{(f)}$ is the static field from the previous image calculation that is normal to the interface. At order ω^1 there is a magnetic field that corresponds to the static electric field according to the equation $\nabla \times \vec{B} = -i\omega E/c$. To compute $\vec{B}^{(f)}$ at this order we again put a dipole $\vec{p} = p\widehat{x}$ at $\vec{r}' = (0,0,d)$ together with its image dipole $-p\widehat{x}$ at $\vec{r}'' = (0,0,-d)$. This corresponds to a current $\vec{J}(\vec{r}) = p\left(\partial\ \delta^3\left(\vec{r} - \vec{r}'\right)/\partial x\right) - p\left(\partial\ \delta^3\left(\vec{r} - \vec{r}''\right)/\partial x\right)$. Computing the magnetic field due to this current we have:

$$B_y^{(f)}(z=0) = \frac{-2ipd\omega}{c\left(\rho^2 + d^2\right)^{3/2}} \text{ and } B_z^{(f)}(z=0) = B_x^{(f)}(z=0) = 0,$$

correct to order ω. $B_y^{(f)}$ is continuous at the interface and $\nabla^2 \vec{B}^{(f)} = -2i\delta^{-2}\vec{B}^{(f)}$ for $z < 0$. The crucial point is that since δ^{-2} is large we may neglect the x and y derivatives in both $\vec{B}^{(f)}$ and $\vec{E}^{(f)}$ for $z < 0$ and we have that

$$B_y^{(f)} = \frac{-2ipd\omega}{c\left(\rho^2 + d^2\right)^{3/2}} \exp\left[(1-i)\, z/\delta\right].$$

Since $\nabla \times \vec{E} = i\omega\vec{B}/c$ for $z < 0$, consistency requires that

$$\frac{\partial E_x^{(f)}}{\partial z} = (1-i)\,\delta^{-1} E_x^{(f)}(z) = i\omega B_y^{(f)}(z)/c$$

at order ω^2. Solving these equations gives

$$E_x^{(f)}(z=0) = \frac{(1+i)\, pd\delta\omega^2}{c^2\left(\rho^2 + d^2\right)^{3/2}}.$$

$E_x^{(f)}$ is continuous at the interface so we also get a correction to the field for $z > 0$ at order ω^2.

For $z > 0$ the field components satisfy the Laplace equation $\nabla^2 \vec{E}^{(f)} = 0$, so we can get the field everywhere by applying Green's theorem to the components of $\vec{E}^{(f)}$:

$$E_x^{(f)}(r) = -\frac{(1+i)\, pd\delta\omega^2}{4\pi c^2} \int dx'dy' \left(\rho'^2 + d^2\right)^{-3/2} \frac{\partial G_D}{\partial n'}$$

where G_D is the Dirichlet Green's function: $G_D = \left|\vec{r} - \vec{r}'\right|^{-1} - \left|\vec{r} - \vec{r}''\right|^{-1}$ and n' is the outward-pointing normal.

Carrying out the integration and using Eq. (23) gives

$$\begin{aligned} \left\langle E_x(\vec{r})\, E_x(\vec{r})\right\rangle_\omega = \left\langle E_y(\vec{r})\, E_y(\vec{r})\right\rangle_\omega &= \frac{\hbar\omega}{8\pi d^2\sigma\delta} \coth\left(\frac{\hbar\omega}{2k_BT}\right) \\ &\approx \begin{cases} \frac{\hbar\omega}{8\pi d^2\sigma\delta} & \text{for } k_BT \ll \hbar\omega \\ \frac{\hbar\omega}{4\pi d^2\sigma\delta} & \text{for } k_BT \gg \hbar\omega. \end{cases} \end{aligned} \tag{44}$$

Since $\delta \sim \frac{1}{\sqrt{\omega\sigma}}$, in the classical limit we have that the noise is proportional to $\sqrt{\omega/\sigma}$, an interesting contrast to the ω/σ dependence in the image regime.

For the z-z correlation function the derivation is only slightly different. We now put a dipole $\vec{p} = p\widehat{z}$ at $\vec{r}' = (0,0,d)$. $\vec{J}(\vec{r}) = p\left(\partial\ \delta^3\left(\vec{r} - \vec{r}'\right)/\partial z\right) + p\left(\partial\ \delta^3\left(\vec{r} - \vec{r}''\right)/\partial z\right)$. The result for the noise spectral density is

$$\left\langle E_z(\vec{r},\omega)\, E_z(\vec{r},\omega)\right\rangle_\omega = \frac{\hbar\omega}{8\pi d^2\sigma\delta} \coth\left(\frac{\hbar\omega}{2k_BT}\right). \tag{45}$$

This is the same as Eq. (44), so the noise becomes isotropic at large distances from a metal surface.

c. Summary of Approximate Results for the Point Qubit. The two regimes are distinguished by the relative magnitudes of d and δ - the distance of the source from the half space and the skin depth. The following physical considerations serve as the basis for understanding electric field noise in small devices.

The image regime of small d/δ is fairly easily understood. In the fictitious problem, the electric field penetrates the metal in the same way it does in the textbook case of two dielectrics of strongly different dielectric constants. The field is strongly screened at the surfaces so that the field lines bend sharply at the interface. Thus the field in the metal is almost parallel to the surface. This field dissipates energy at the usual rate $\sim \sigma \left|\vec{E}\right|^2$ per unit volume in the fictitious problem, and the physical fluctuations are also proportional to this. However, the "impedance mismatch" dominates to the extent that $\left|\vec{E}\right| \sim 1/\sigma$ in the metal overall and the noise spectral density at a given frequency is proportional to $1/\sigma$. The noise is stronger for poor conductors since the field penetrates further. Once the dependence on the conductivity has been determined, the $1/d^3$ spatial dependence follows by dimensional analysis or noting that the fictitious field is produced by an image dipole.

The induction regime of large d/δ is somewhat different. The electric field is essentially normal to the interface. This induces a magnetic field parallel to the interface which penetrates only a distance δ into the metal. This in turn induces an electric field that dissipates energy. The volume in which the energy is dissipated is of thickness δ rather than d, so the dissipation is proportional to δ. Thus the image result is reduced by the factor δ/d, and the noise spectral density is proportional to $1/d^2\sqrt{\sigma}$.

4.1.2. Extended Qubits

For extended qubits, we need the full $\vec{r}$ and $\vec{r}'$ dependence of G. We compute using a method that will be used repeatedly in what follows. Details are given in the Appendix, along with explicit forms for the off-diagonal components of the noise tensors. We place a fictitious dipole $\vec{p} = p\hat{z}$ at $\vec{r}' = (0,0,d)$ and find the induced field

$$\vec{E}^{(ind)}(\vec{r}) = -\frac{p}{2\pi}\int d^2q\ \left(-iq_x, -iq_y, q\right)\ e^{-qd} \times \frac{1-(\varepsilon_m/\varepsilon_d)\,q/\alpha}{1+(\varepsilon_m/\varepsilon_d)\,q/\alpha} e^{i\vec{q}\cdot\vec{\rho}} e^{-qz}$$

for $z > 0$, and the corresponding electric noise is given by Eq. (23):

$$\left\langle \vec{E}\left(\vec{r} = (\vec{\rho}, z)\right) E_z\left(\vec{r}' = (0,0,d)\right)\right\rangle_\omega = -\frac{\hbar}{2\pi}\coth\frac{\hbar\omega}{2k_BT} \times \mathrm{Im}\int d^2q\ \left(-iq_x, -iq_y, q\right)\ e^{-qd}\frac{1-(\varepsilon_m/\varepsilon_d)\,q/\alpha}{1+(\varepsilon_m/\varepsilon_d)\,q/\alpha} e^{i\vec{q}\cdot\vec{\rho}} e^{-qz} \tag{46}$$

The integral is complicated, but it can be evaluated numerically and it simplifies in the limits of large and small d. When $d \ll \delta$, $\alpha \approx q$ and we find for the physical noise

$$\left\langle \vec{E}(\vec{r})\, E_z(\vec{r}')\right\rangle_\omega \approx -\frac{\hbar\omega\varepsilon_d}{2\pi\sigma}\coth\frac{\hbar\omega}{2k_BT}\nabla\frac{d+z}{\left[(d+z)^2+\rho^2\right]^{3/2}}$$

The diagonal component is

$$\langle E_z(\vec{r})\, E_z(\vec{r}')\rangle_\omega = \frac{\hbar\omega\varepsilon_d}{2\pi\sigma}\coth\frac{\hbar\omega}{2k_BT}\frac{2(d+z)^2-\rho^2}{\left[(d+z)^2+\rho^2\right]^{5/2}},$$

and it can be verified that this equation reduces to Eq. (43) when $\vec{r} = \vec{r}' = (0,0,d)$, an important check. This case has the unusual feature of anticorrelations in E_z for large lateral separations of $\vec{r} - \vec{r}'$: $\rho > \sqrt{2}\,(d+z)$. This implies that in the appropriate geometry there can be cancellations in the integral that determines qubit decoherence. This can be incorporated as a design feature.

For $d \gg \delta$ (but still $d \ll \delta\sigma/\omega$) we have $\alpha \approx (1-i)\,\delta^{-1}$ and the physical noise correlation function is

$$\left\langle \vec{E}(\vec{r})\, E_z(\vec{r}')\right\rangle_\omega = -\frac{\hbar\omega\varepsilon_d}{2\pi\sigma\delta}\coth\frac{\hbar\omega}{2k_BT}\nabla\frac{1}{\left[(d+z)^2+\rho^2\right]^{1/2}}$$

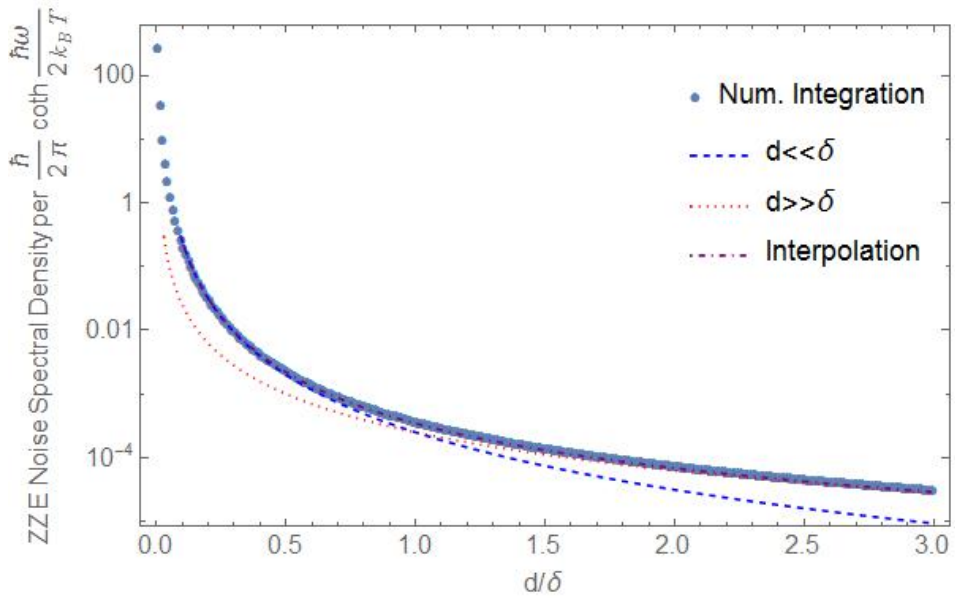

FIG. 4: Numerical integration of Eq. (46), the electric noise spectral density for a localized qubit in the half-space geometry, compared with image and induction regime approximate results. $\frac{\sigma}{\omega}=100$ and $p=2.17$ for the interpolated function Eq. (47).

Specializing to the zz correlation function,

$$\left\langle E_z\left(\vec{r}\right)E_z\left(\vec{r}'\right)\right\rangle_\omega=\frac{\hbar\omega\varepsilon_d}{2\pi\sigma\delta}\coth\frac{\hbar\omega}{2k_BT}\frac{d+z}{\left[\left(d+z\right)^2+\rho^2\right]^{3/2}},$$

and it can be verified that this equation reduces to Eq. 45 when $\vec{r}=\vec{r}'=(0,0,d)$. The situation for $\langle\vec{E}(r)E_x(r')\rangle_\omega$ is somewhat more complicated because of the lack of cylindrical symmetry. However, the method of the previous section does not depend on the symmetry and it can still be used. We now use $\vec{p}=p\hat{x}$. This leads to a fictitious induced electric field for $z>0$:

$$\vec{E}^{(ind)}\left(\vec{r}\right)=-\frac{p}{2\pi}\frac{\partial}{\partial x}\nabla\int d^2q\ \frac{1}{q}e^{-q(d+z)}\frac{1-\left(\varepsilon_m/\varepsilon_d\right)q/\alpha}{1+\left(\varepsilon_m/\varepsilon_d\right)q/\alpha}e^{iq_xx+iq_yy}$$

and the physical noise correlation is

$$\left\langle\vec{E}\left(\vec{r}\right)E_x\left(\vec{r}'\right)\right\rangle_\omega=-\frac{\hbar}{2\pi}\frac{\partial}{\partial x}\nabla\int d^2q\ e^{-q(d+z)}\,\mathrm{Im}\frac{1-\left(\varepsilon_m/\varepsilon_d\right)q/\alpha}{1+\left(\varepsilon_m/\varepsilon_d\right)q/\alpha}e^{iq_xx+iq_yy}\coth\frac{\hbar\omega}{2k_BT}.$$

For $d\ll\delta$ we have diagonal element of the physical noise spectral density

$$\left\langle E_x\left(\vec{r}\right)E_x\left(\vec{r}'\right)\right\rangle_\omega=-\frac{\hbar}{2\pi}\frac{\omega\varepsilon_d}{\sigma}\frac{2x^2-\left(z+d\right)^2-y^2}{\left[\left(z+d\right)^2+\rho^2\right]^{5/2}}\coth\frac{\hbar\omega}{2k_BT},$$

in agreement with Eq. (42). At $\vec{r}=\vec{r}'$ we find

$$\left\langle E_x\left(\vec{r}\right)E_x\left(\vec{r}=\vec{r}'\right)\right\rangle_\omega=\frac{\hbar}{16\pi}\frac{\omega\varepsilon_d}{\sigma d^3}\coth\frac{\hbar\omega}{2k_BT}.$$

In the high T limit this reduces to

$$\left\langle E_x\left(\vec{r}\right)E_x\left(\vec{r}=\vec{r}'\right)\right\rangle_\omega=\frac{k_BT\varepsilon_d}{8\pi\sigma d^3}.$$

For $d \gg \delta$ (but still $d \ll \delta\omega/\sigma$) we have

$$\left\langle \vec{E}\left(\vec{r}\right) E_x\left(\vec{r}\right)\right\rangle_\omega = \frac{\hbar}{2\pi}\frac{\omega\varepsilon_d}{\sigma\delta}\nabla\left\{\frac{x}{\rho^2}\left[1-\frac{d+z}{\left[\left(z+d\right)^2+\rho^2\right]^{1/2}}\right]\right\}\coth\frac{\hbar\omega}{2k_BT},$$

and the various components of the tensor may be calculated from this expression.

We have

$$\left\langle E_x\left(\vec{r}\right) E_x\left(\vec{r}'\right)\right\rangle_\omega = \frac{\hbar}{2\pi}\frac{\omega\varepsilon_d}{\sigma\delta}\coth\frac{\hbar\omega}{2k_BT}\times \left\{\frac{y^2-x^2}{\rho^4}\left[1-\frac{d+z}{\left[\left(z+d\right)^2+\rho^2\right]^{1/2}}\right]+\frac{x^2\left(d+z\right)}{\rho^2\left[\left(z+d\right)^2+\rho^2\right]^{3/2}}\right\}$$

and in particular at $\vec{r}=\vec{r}'$ we find

$$\left\langle E_x\left(\vec{r}\right) E_x\left(\vec{r}\right)\right\rangle_\omega = \frac{\hbar\omega\varepsilon_d}{16\pi\sigma\delta d^2}\coth\frac{\hbar\omega}{2k_BT},$$

which is in agreement with Eq. (44).

4.1.3. Between Induction and Image Regimes

In general Eq. (46) cannot be simplified, but in both the image and induction regime we can find analytic results (Eqs. (43) and (45)). Using these two results, we can interpolate a function to compute correlation functions for qubit geometries that do not fall into either of the extremal cases treated here. For two functions f_1 and f_2 we define a family of interpolated functions

$$f_{int}(p) = \left(f_1^p + f_2^p\right)^{\frac{1}{p}} \tag{47}$$

and search for the $p \in \mathbb{R}$ that optimizes the interpolated function's agreement with the extended qubit noise spectral density. The interpolated functions are plotted alongside numerical results for Eqs. (46) and (51) in Fig. 4 and Fig. 6 respectively.

4.2. Conducting Cylinder

We consider a infinite conducting circular cylinder (conductivity σ and radius a) with its axis along the z-direction. There is a qubit at the point $\vec{r}' = (d, 0, 0)$. We wish to compute $\langle B_i\left(\vec{r}'\right) B_i\left(\vec{r}'\right)\rangle$ with $i = x, y, z$. We're particularly interested in the anisotropy of relaxation times, which depend on the ratios of this correlation function for different values of i. The most common case is when the skin depth $\delta \gg a$. We will also be mainly interested in thin wires also in the sense that $d \ll a$. This means that the fictitious applied field is slowly varying over the cylinder. The the problem reduces to a computation of the electric polarizability.

The problem of the *magnetic* polarizability of a conducting cylinder in a uniform field is a standard one [35]. We modify the solution to obtain the electric polarizability $\vec{\beta}$, defined by $P_i = \pi a^2 \beta_i E_i$, where P_i is the electric dipole moment per unit length in direction i. We find

$$\beta_x = \frac{1}{2\pi}\frac{4\pi i\sigma/\omega - C}{4\pi i\sigma/\omega + C}$$

with

$$C = -1 + \frac{kaJ_0\left(ka\right)}{J_1\left(ka\right)}.$$

and $k = \left(1+i\right)/\delta$.

Again, the most interesting case is when $\delta \gg a$, so $|ka| \ll 1$ and

$$\frac{kaJ_0(ka)}{J_1(ka)} \approx ka\frac{1}{ka/2} = 2,$$

and then we find

$$\mathrm{Im}\,\beta_x = \frac{\omega}{\pi\sigma}.$$

When $d \gg a$ we can integrate along the z-axis assuming uniform applied field. Some further details are given in Sec. 4. We find

$$\langle E_x(\vec{r}')\,E_x(\vec{r}')\rangle = \frac{123\omega\hbar a^2}{256\sigma d^5}\coth\left(\frac{\hbar\omega}{2k_BT}\right)$$

and

$$\langle E_y(\vec{r}')\,E_y(\vec{r}')\rangle = \frac{3\omega\hbar a^2}{32\sigma d^5}\coth\left(\frac{\hbar\omega}{2k_BT}\right).$$

We may calculate the noise correlation for the z-direction in the same way. However, this would seem to be problematic, since in a any finite wire the electric flux would scome through the ends. We present the result as a conjecture to be investigated in further work:

$$\langle E_z(\vec{r}')\,E_z(\vec{r}')\rangle = \frac{27\pi\hbar a^4}{2048d^5\delta^2}\coth\left(\frac{\hbar\omega}{2k_BT}\right).$$

4.3. Distant Object

We now treat the electrical noise of a metallic object far away from the qubit ($d \gg L$). We consider a fictitious point dipole $\vec{p}$ at $\vec{r}'$, the metallic object approximated by a sphere at the origin and an observation point $\vec{r}$. Eq. (17) gives the correlation function:

$$\langle E_i(\vec{r})\,E_k(\vec{r}')\rangle = \hbar\coth\left(\frac{\hbar\omega}{2k_BT}\right)$$
$$\times\,\mathrm{Im}\left[\alpha(\omega)\right]\frac{9x_ix'_k\;\vec{r}\cdot\vec{r}' + \delta_{ik}r^2r'^2 - 3x_ix_kr'^2 - 3x'_ix'_kr^2}{r^5r'^5},$$

where now $\vec{E}$ is the physical fluctuating field. The local noise at $\vec{r}$ is

$$\langle E_i(\vec{r})\,E_k(\vec{r}'=\vec{r})\rangle = \hbar\coth\left(\frac{\hbar\omega}{2k_BT}\right)\mathrm{Im}\,(\alpha)\,\frac{3x_ix_k+\delta_{ik}r^2}{r^8}. \tag{48}$$

The r^{-6} dependence is familiar from the van der Waals force, which has a similar physical origin.

The *anisotropy* in lifetimes of a qubit in the presence of a spherical electrode is independent of the value of α. If the qubit is located at $\vec{r} = r\widehat{z}$, then

$$\langle E_x(\vec{r})\,E_x(\vec{r})\rangle = \langle E_y(\vec{r})\,E_y(\vec{r})\rangle = \hbar\coth\left(\frac{\hbar\omega}{2k_BT}\right)\frac{\mathrm{Im}\left[\alpha(\omega)\right]}{r^6}$$
$$\langle E_z(\vec{r})E_z(\vec{r})\rangle = 4\hbar\coth\left(\frac{\hbar\omega}{2k_BT}\right)\frac{\mathrm{Im}\left[\alpha(\omega)\right]}{r^6}.$$

The anisotropy

$$\langle E_z(\vec{r})\,E_z(\vec{r})\rangle = 4\,\langle E_x(\vec{r})\,E_x(\vec{r})\rangle$$

is stronger than in the half-space case. Thus the problem of noise from a distant metallic object reduces to a calculation of $\mathrm{Im}\left[\alpha(\omega)\right]$, the dissipative part of the polarizability of the electrode. To get α, we need to calculate the change in the charge density of the electrode due to a distant oscillating dipole, and the electric field that results from this charge. We do this now in two limits.

a. Image Regime We first consider a metallic sphere of radius a with $\delta \gg a$. Once again the fictitious problem is mathematically identical with that of a dielectric sphere in a static field, so we may simply transcribe the textbook formulas for the polarizability:

$$\alpha = \frac{\varepsilon_m/\varepsilon_d - 1}{\varepsilon_m/\varepsilon_d + 2} a^3 \approx \left(1 + \frac{3i\omega\varepsilon_d}{4\pi\sigma}\right) a^3. \tag{49}$$

Hence

$$\langle E_i(\vec{r})\, E_k(\vec{r})\rangle = \frac{3\hbar\omega\varepsilon_d a^3}{4\pi\sigma} \frac{3x_i x_k + \delta_{ik} r^2}{r^8} \coth\left(\frac{\hbar\omega}{2k_B T}\right)$$

For a metallic ellipsoid with radii a_x, a_y, a_z in the x, y, z directions the coordinate system is aligned with the axes of the ellipsoid and the polarizability tensor satisfies $\alpha_{ij} = \delta_{ij}\alpha_{ii}$ with

$$\begin{aligned}\alpha_{ii} &= \frac{1}{3} \frac{\varepsilon_m/\varepsilon_d - 1}{1 + (\varepsilon_m/\varepsilon_d - 1)\, n_i} a_x a_y a_z \\ &\approx \left(1 + \frac{i\omega\varepsilon_d}{12 n_i^2 \pi\sigma}\right) a_x a_y a_z.\end{aligned}$$

The depolarizing factors n_x, n_y, n_z are positive and satisfy $n_x + n_y + n_z = 1$ and n_i are decreasing functions of a_i. In particular, if $a_x < a_y < a_z$ then $n_x > n_y > n_z$. The connection between the n_i and the a_i involves elliptic integrals. Exact expressions and tables may be found in [36]. Using Eq. (B6) we have

$$\begin{aligned}\langle E_i(\vec{r})\, E_k(\vec{r}')\rangle &= \hbar \coth\left(\frac{\hbar\omega}{2k_B T}\right) \mathrm{Im}\left(\alpha_{jj}\right) f_{kj}(\vec{r}')\, f_{ij}(\vec{r}) \\ &= \frac{\hbar\omega\varepsilon_d V}{16\pi^2\sigma} \coth\left(\frac{\hbar\omega}{2k_B T}\right) \times \frac{1}{n_j^2} \frac{3x'_k x'_j - \delta_{kj} r'^2}{r'^5} \frac{3x_i x_j - \delta_{ij} r^2}{r^5},\end{aligned}$$

a distance r from the center of the ellipsoid of volume V. To understand the physics of this formula, think of a qubit at $\vec{r} = r\hat{z}$ with the origin of coordinates at the center of the ellipsoid. Then the off-diagonal components of the noise tensor vanish and the formula exhibits the anisotropy mentioned above. This expression confirms the intuition that the noise should be stronger in the directions where the axis is longer, since the polarizability is greater.

b. Induction regime Again we first consider a metallic sphere of radius a. The electric field outside the sphere in lowest order in ω in spherical coordinates is

$$\vec{E}^{(0)} = \hat{r} E_0 \left(1 + \frac{2a^3}{r^3}\right) \cos\theta - \hat{\theta} E_0 \left(1 - \frac{a^3}{r^3}\right) \sin\theta$$

and solving the equation $\nabla \times \vec{B}^{(0)} = i\lambda^{-1}\vec{E}^{(0)}$ we get a corresponding magnetic field

$$\vec{B}^{(0)}_{out} = -\frac{iE_0}{2\lambda} \left(r + \frac{2a^3}{r^2}\right) \sin\theta\ \hat{\phi}$$

and using this as a boundary condition for the solution of the diffusion equation inside the sphere gives

$$\vec{B}^{(0)}_{in} = -\frac{3iE_0 a}{2\lambda} \sin\theta\ e^{-(1-i)(a-r)/\delta}\ \hat{\phi}$$

where again the condition $\delta \ll a$ has been used to neglect the tangential derivatives. Since $\vec{E}_{in} = (c/4\pi\sigma)\nabla \times \vec{B}_{in}$ this gives an electric field

$$\begin{aligned}\vec{E}^{(1)}_{in} &= -\hat{\theta}\,(c/4\pi\sigma) \left(-\frac{3iE_0 a}{2\lambda}\right) \sin\theta \frac{1}{r} \left[\frac{\partial}{\partial r} r e^{-(1-i)(a-r)/\delta}\right] \\ &= \hat{\theta} \left(\frac{3\,(1+i)\, E_0 \omega a}{8\pi\sigma\delta}\right) \sin\theta\ e^{-(1-i)(a-r)/\delta},\end{aligned}$$

and since this field is tangential it is continuous at the boundary we can simply compare this field with the field of a dipole in the z-direction: $\vec{E}_{dip} = \left(p\sin\theta/a^3\right)\hat{\theta}$, together with $p = \alpha E_0$ and we find

$$\alpha = \frac{3\,(1+i)\,\omega a^4}{8\pi\delta\sigma}$$

for the polarizability in the induction regime. Using Eq. (48), we have that if the qubit is located at $\vec{r} = r\widehat{z}$, then

$$\langle E_x\left(\vec{r} = r\widehat{z}\right) E_x\left(\vec{r} = r\widehat{z}\right)\rangle = \langle E_y\left(\vec{r} = r\widehat{z}\right) E_y\left(\vec{r} = r\widehat{z}\right)\rangle = \frac{3\hbar\omega a^4}{8\pi\sigma\delta r^6}\coth\left(\frac{\hbar\omega}{2k_BT}\right)$$

$$\langle E_z\left(\vec{r} = r\widehat{z}\right) E_z\left(\vec{r} = r\widehat{z}\right)\rangle = \frac{3\hbar\omega a^4}{2\pi\sigma\delta r^6}\coth\left(\frac{\hbar\omega}{2k_BT}\right).$$

c. General result The problem of the polarization of a metallic sphere is exactly solvable for all d/δ but it is not trivial. The method may be found in [37], and it is discussed in [38], but seems not to have been solved previously!

The polarizability α for the sphere of radius a is given by

$$a^{-3}\alpha = -\frac{1}{2}\frac{\kappa^2 a\ j_0 + (1+2\varepsilon)\ j_0'}{\kappa^2 a\ j_0 + (1-\varepsilon)\ j_0'}.$$

The symbols are defined as $\kappa = (1+i)/\delta$, $j_0 = (1/\kappa a)\sin\kappa a$, $j_0' = (1/a)\cos\kappa a - \left(1/\kappa a^2\right)\sin\kappa a$.

To obtain the first correction in the case $\delta \gg a$ we expand to first order in ω/σ and a/δ, (always assuming $\omega/\sigma \ll a/\delta$) and find

$$j_0 \approx 1,\ j_0' \approx -\frac{1}{3}\kappa^2 a$$

and we have

$$\alpha = a^3\left(1 + \frac{3i\omega}{4\pi\sigma}\right),$$

in agreement with Eq. (49) for the dissipative part. Note that the term that is zeroth-order in ω gives a polarizability $\alpha = a^3$, which is the proper static limit given in many textbooks.

When $\delta \ll a$, then

$$j_0 \approx \frac{i}{2\kappa a}e^{-i(1+i)a/\delta}, \quad j_0' \approx \frac{1}{2a}e^{-i(1+i)a/\delta}$$

and

$$\alpha \approx a^3\left(1 + \frac{3a\,(1+i)\,\omega}{8\pi\sigma\delta}\right).$$

As ω increases, we find that $\operatorname{Im}\alpha$ increases, so it is a monotonic function of ω.

4.4. Multiple Objects

Real devices tend to have complex geometries with multiple metallic device elements. A modern spin qubit experiment may involve a back gate or an accumulation gate having a layer or half-space shape. There may be up to tens of finger gates for lateral or voltage control that are approximately cylindrical. Clearly a numerical approach is indicated for these cases, which is beyond the scope of this paper. We therefore limit ourselves to a few remarks.

In many cases, it may be reasonable to regard different metallic elements as noise sources that are statistically independent. If this assumption holds, then

$$\langle E_i\left(\vec{r}\right) E_j\left(\vec{r}'\right)\rangle_\omega = \sum_{s=1}^{N}\langle E_i\left(\vec{r}\right) E_j\left(\vec{r}'\right)\rangle_\omega^{(s)}, \tag{50}$$

where the (s) indexes the sources, of which there are N total. The various noise sources add incoherently.

The physical analogy of Sec. 2 shows that this assumption cannot be be strictly correct. The various device elements are in fact all driven by a single fictitious dipole and they are therefore in phase. However, unless the qubit occupies a position of high symmetry with regard to at least one pair of metallic objects. This can occur: it is common to place qubits near the tips of opposing finger gates. However, in most other cases the symmetry is low and Eq. (50) can be used.

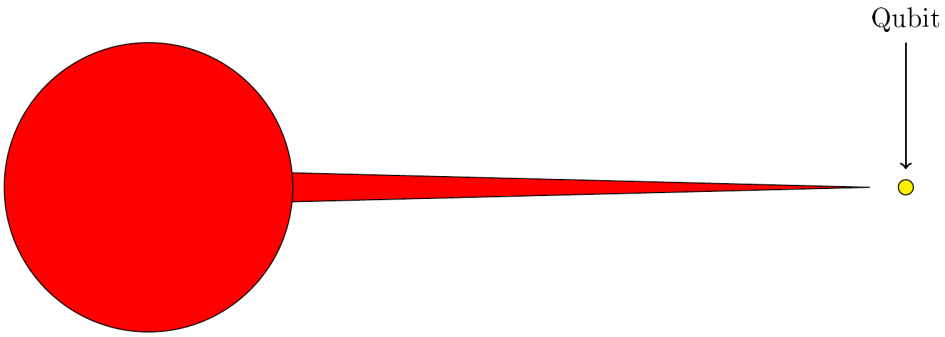

FIG. 5

4.5. Sharp Points

A serious concern for qubit decoherence is the geometrical enhancement of noise in the neighborhood of surface asperities of conductors. The question is whether the well-known divergence of local field strengths at such structures carries over to noise. This is a particularly pressing issue for for semiconductor qubits where finger gates with sharp points are a standard feature of device architectures. However, it can be seen fairly simply that electric noise is not greatly enhanced by asperities in the case that δ is greater than the size of the surface feature (the usual case). We imagine a spherical geometry with a sharp point added on top, and a qubit near the point (See Fig. 5). Qualitatively, the quasistatic electric field lines will gather at the point, giving the familiar lightning-rod effect. However, these lines are outside the object and they do not produce the dissipation that is associated with field fluctuations and noise. Inside, the magnitude of the field is reduced by a factor ω/σ. This internal field produces currents and it is therefore the field associated with the dissipative part of the response, and, in turn, to the noise strength. These currents run away from the point and give rise to the surface charge $\sigma\left(\vec{r}'\right)$ whose density diverges at the tip as $r^{-1+\nu}$, $\nu = \left[2\ln\left(2/\alpha\right)\right]^{-1}$, where α is half the opening angle of the tip, taken here as a cone (*i.e.,* $\alpha = 0$ for an infinitely sharp tip). The presence of the logarithm means that $\nu \ll 1$ even for a very sharp tip. Note $\nu > 0$.

The z component of the fictitious electric field at the point $\vec{r} = (0, 0, -d)$ is proportional to

$$\begin{aligned} E_z^{(f)}\left(\vec{r}\right) &\sim \int_0^p d^2r' \frac{\sigma\left(\vec{r}'\right)\left(\vec{r}-\vec{r}'\right)_z}{\left|\vec{r}-\vec{r}'\right|^3} \\ &\sim \int_0^p \sin\alpha\; r' dr' \frac{\left(r'\right)^{-1+\nu}\left(-d - r'\cos\alpha\right)}{\left|\left(r'\right)^2 + d^2 + 2dr'\cos\alpha\right|^{3/2}} \end{aligned}$$

where p is an upper cutoff on the size of the cone. We are only interested in the small d behavior, which follows from simple scaling arguments as $E_z^{(f)} \sim d^{\nu+1/2}$ and this carries over to the physical field fluctuations $\left\langle E_z\left(\vec{r}\right) E_z\left(\vec{r}\right)\right\rangle_\omega \sim d^{\nu+1/2}$. So the divergence of the fields as the point is approached along the surface does not carry over to the noise in the immediate region near the tip but outside the conductor.

4.6. Charge qubits

To understand qubit decoherence in the presence of noise, the frequency dependence of the noise is of paramount importance. To this end, write the noise spectral density $\left\langle E_i\left(\vec{r}\right) E_j\left(\vec{r}'\right)\right\rangle$from EWJN as

$$\left\langle E_i\left(\vec{r}\right) E_j\left(\vec{r}'\right)\right\rangle_\omega = f\left(\omega\right)\;\omega\;\coth\left(\frac{\hbar\omega}{2k_BT}\right),$$

where all spatial and device geometry information is contained in $f\left(\omega\right)$. For EWJN, $f\left(\omega\right) \to f_0$, a constant as $\omega \to 0$. f_0 sets the overall scale of the noise strength. In addition there is a high-frequency cutoff $1/\tau$ at the relaxation time for the conduction electrons in the metal. Thus $f\left(\omega\right) \to 0$ when $\omega \gg 1/\tau$. Physically, the factor of ω comes from the connection of noise to dissipation. Photons are non-interacting bosons - hence the cotangent factor. This sort of noise is white, or at least white-ish. This means that echo techniques are not likely to be very useful for extending

qubit lifetimes when EWJN is the dominant source of decoherence. This noise is essentially the same as that of the well-known spin-boson model and the results are well known, so we only briefly summarize results here and give no derivations.

There are three frequency regime for the spectral density. 1. When $0 \leq \omega < 2k_BT/\hbar$, then $\langle E_i(\vec{r})\, E_j(\vec{r}')\rangle_\omega = 2k_BTf_0/\hbar$. 2. When $2k_BT/\hbar < \omega < 1/\tau$ we have $\langle E_i(\vec{r})\, E_j(\vec{r}')\rangle = f(\omega)\ \omega$, where typically the frequency dependence of $f(\omega)$ is weak. 3. When $\omega > 1/\tau$, then the frequency dependence is material-dependent but we may usually assume that the noise is cut off.

In regime 1, the fluctuations are thermal. Regime 2 is the quantum regime and the linear spectrum is refered to as "ohmic". Regime 3 is above the the high-frequency cutoff, whose presence is implicit in this paper. The symbol σ denotes the DC conductivity; however, no equation in which it appears can be used at frequencies greater than $1/\tau$. This frequency range is generally in the infrared for metals.

The qubit energy level separation is $\hbar\omega_0$ and ω_0 may be in either Regime 1 or Regime 2, depending on the implementation. No existing implementation operates in Regime 3.

5. MAGNETIC NOISE

5.1. Half Space

For magnetic noise the image method is not useful, so we proceed directly to general results for extended qubits.

5.1.1. Extended Qubits

Again, we are interested in a metal with conductivity σ that occupies the half space $z < 0$. The equations satisfied by the fields are the same as for the electric case. The only difference for magnetic fields is that $\vec{B}$, unlike E, is continuous at the interface, since we dealing with non-magnetic materials.

For this problem we place a fictitious magnetic dipole moment $\vec{m}$ at the point $\vec{r}' = (0, 0, d)$ and the physical noise spectral density is

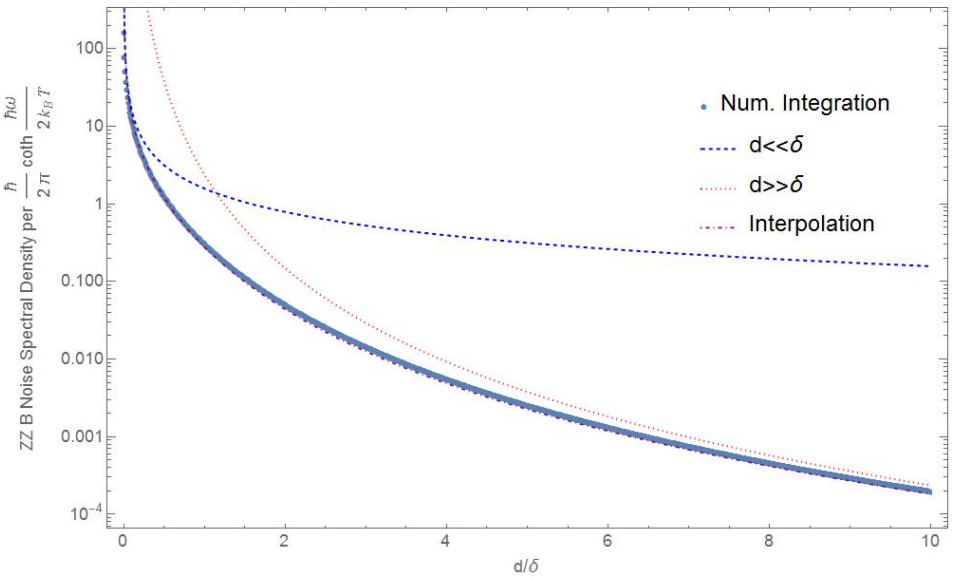

FIG. 6: Numerical integration of Eq. (51), the magnetic noise spectral density for a localized qubit in the half-space geometry, compared with image and induction regime approximate results. $\frac{\sigma}{\omega} = 100$ and $p = -0.358$ for the interpolated function Eq. (47).

$$\left\langle \vec{B}\left(\vec{r}\right) B_z\left(\vec{r}'\right)\right\rangle_\omega = \frac{\hbar}{4\pi\delta^2}\coth\frac{\hbar\omega}{2k_BT}\,\mathrm{Im}\int d^2q\frac{1}{q^2}\;\left(q_x,q_y,iq\right)e^{-q(z+d)}e^{iq_xx+iq_yy} \tag{51}$$
$$= -\frac{\hbar}{4\pi\delta^2}\coth\frac{\hbar\omega}{2k_BT}\nabla\int d^2q\frac{1}{q^2}e^{-q(z+d)}e^{iq_xx+iq_yy}$$

The diagonal element is

$$\left\langle B_z\left(\vec{r}\right)B_z\left(\vec{r}'\right)\right\rangle_\omega = \frac{\hbar}{4\pi\delta^2}\coth\frac{\hbar\omega}{2k_BT}\int d^2q\frac{1}{q}e^{-q(z+d)}e^{iq_xx+iq_yy}$$
$$= \frac{\hbar}{2\delta^2}\frac{1}{\left[\left(d+z\right)^2+\rho^2\right]^{1/2}}\coth\frac{\hbar\omega}{2k_BT},$$

and off-diagonal components are in the appendix.

For a point qubit ($\vec{r}=\vec{r}'$) we have

$$\left\langle B_z\left(\vec{r}\right)B_z\left(\vec{r}\right)\right\rangle_\omega = \frac{\hbar}{4d\delta^2}\coth\frac{\hbar\omega}{2k_BT}.$$

And in the high T limit this reduces to

$$\left\langle B_z\left(\vec{r}\right)B_z\left(\vec{r}\right)\right\rangle_\omega = \frac{k_BT}{2\omega d\delta^2}.$$

For $d\gg\delta$ we have

$$\frac{1-q/\alpha}{1+q/\alpha}\approx\left(1+q\delta+iq\delta\right),$$

and

$$\left\langle \vec{B}\left(\vec{r}\right)B_z\left(\vec{r}'\right)\right\rangle_\omega = -\frac{\hbar\delta}{2\pi}\coth\frac{\hbar\omega}{2k_BT}\nabla\int d^2q\;q\;e^{-q(z+d)}e^{iq_xx+iq_yy}$$

The diagonal component is

$$\left\langle B_z\left(\vec{r}\right)B_z\left(\vec{r}'\right)\right\rangle_\omega = -\hbar\delta\coth\frac{\hbar\omega}{2k_BT}\times\left[\frac{-6\left(z+d\right)^3+9\rho^2\left(z+d\right)}{\left[\left(d+z\right)^2+\rho^2\right]^{7/2}}\right],$$

For a point qubit only the diagonal component is nonzero:

$$\left\langle B_z\left(\vec{r}\right)B_z\left(\vec{r}\right)\right\rangle_\omega = \frac{3\hbar\delta}{8d^4}\coth\frac{\hbar\omega}{2k_BT}.$$

5.1.2. Solution for $\vec{m}=m\widehat{x}$.

This is more complicated because of the lack of cylindrical symmetry, but the essential procedure is the same. We find

$$\left\langle \vec{B}\left(\vec{r}\right)B_x\left(\vec{r}'\right)\right\rangle_\omega = \frac{\hbar}{2\pi}\coth\frac{\hbar\omega}{2k_BT}\frac{\partial}{\partial x}\nabla\,\mathrm{Im}\int d^2q\;\frac{1}{q}\frac{1-q/\alpha}{1+q/\alpha}e^{iq_xx+iq_yy-q(z+d)}$$

For $d\ll\delta$ this is

$$\left\langle \vec{B}\left(\vec{r}\right)B_x\left(\vec{r}'\right)\right\rangle_\omega = -\frac{\hbar}{2\delta^2}\coth\frac{\hbar\omega}{2k_BT}\frac{\partial}{\partial x}\nabla\int_0^\infty dq\;\frac{1}{q^2}e^{-q(z+d)}J_0\left(q\rho\right)$$

The diagonal component is

$$\left\langle B_x\left(\vec{r}\right)B_x\left(\vec{r}'\right)\right\rangle_\omega = \frac{\hbar}{2\delta^2}\coth\frac{\hbar\omega}{2k_BT}\left[\frac{x^2-y^2}{\rho^2}\left\{\left[\left(d+z\right)^2+\rho^2\right]^{1/2}-\left(d+z\right)\right\}-\frac{x^2}{\rho^2\left[\left(d+z\right)^2+\rho^2\right]^{1/2}}\right].$$

At $\vec{r}=\vec{r}'$ we have that only the diagonal component is non-vanishing and

$$\langle B_x(\vec{r}')\,B_x(\vec{r}')\rangle=\frac{\hbar}{8d\delta^2}\coth\frac{\hbar\omega}{2k_BT}.$$

In the high T limit this reduces to

$$\langle B_x(\vec{r}')\,B_x(\vec{r}')\rangle=\frac{k_BT}{4d\omega\delta^2}.$$

For $d\gg\delta$ we get

$$\left\langle\vec{B}(\vec{r})\,B_x(\vec{r}')\right\rangle_\omega=-\hbar\delta\coth\frac{\hbar\omega}{2k_BT}\frac{\partial}{\partial x}\nabla\frac{\partial}{\partial z}\frac{1}{\left[(d+z)^2+\rho^2\right]^{1/2}}.$$

This yields

$$\langle B_x(\vec{r})\,B_x(\vec{r}')\rangle_\omega=\hbar\delta\coth\frac{\hbar\omega}{2k_BT}(d+z)\frac{3(d+z)^2+3\rho^2-15x^2}{\left[(d+z)^2+\rho^2\right]^{7/2}}$$

For $\vec{r}=\vec{r}'$ only the diagonal component is nonzero:

$$\langle B_x(\vec{r}')\,B_x(\vec{r}')\rangle_\omega=\frac{3\hbar\delta}{16\pi d^4}\coth\frac{\hbar\omega}{2k_BT}.$$

In the high T limit this becomes

$$\langle B_x(\vec{r}')\,B_x(\vec{r}')\rangle_\omega=\frac{3\hbar\delta}{8\pi d^4}.$$

5.2. Cylinder

In this section, we consider a infinitely long conducting circular cylinder as a source of EWJN. The cylinder has conductivity σ and radius a and its axis is along the z-direction. This geometry is important, since cylindrical microwave antennas are used for single qubit rotations. There is a qubit at the point $\vec{r}'=(d,0,0)$. We wish to compute $\langle B_i(\vec{r}')\,B_i(\vec{r}')\rangle$ with $i=x,y,z$. We're particularly interested in the anisotropy of relaxation times, which depend on the ratios of this correlation function for different values of i. The most common case is when the skin depth $\delta\gg a$. We will also be mainly interested in thin wires also in the sense that $d\gg a$.

We need the solution to the problem of the magnetic polarizability of a conducting cylinder in a uniform field. This is given by [35]. The polarizabilities α_i are defined by the formulas

$$\begin{aligned}M_x&=\pi a^2\alpha_xB_x\\M_y&=\pi a^2\alpha_yB_y\\M_z&=\pi a^2\alpha_zB_z,\end{aligned}$$

where M_i is the magnetic moment per unit length in direction i. Here

$$\begin{aligned}\alpha_x=\alpha_y&=-\frac{1}{2\pi}\left[1-\frac{2}{ka}\frac{J_1(ka)}{J_0(ka)}\right],\\\alpha_z&=-\frac{1}{4\pi}\left[1-\frac{2}{ka}\frac{J_1(ka)}{J_0(ka)}\right],\end{aligned}$$

with $k=(1+i)/\delta$. We will mainly need the imaginary part in the limit where $\delta\gg a$, which is

$$\begin{aligned}\operatorname{Im}\alpha_x=\operatorname{Im}\alpha_y&=\frac{a^2}{8\pi\delta^2}\\\operatorname{Im}\alpha_z&=\frac{a^2}{16\pi\delta^2}.\end{aligned}$$

For illustration purposes we give some details of the calculation for $i = j = z$.
The fictitous dipole $\vec{m} = m\hat{z}$ at the point $\vec{r}' = (d, 0, 0)$ sets up a field

$$B_z(\vec{r}) = m\frac{3(\vec{r}-\vec{r}')_z(\vec{r}-\vec{r}')_z - \delta_{zz}|\vec{r}-\vec{r}'|^2}{|\vec{r}-\vec{r}'|^5}$$

and along the axis of the cylinder this is

$$B_z(\vec{r} = (0,0,z)) = m\frac{2z^2-d^2}{(z^2+d^2)^{5/2}}.$$

Note that this changes sign as a function of z, which is a characteristic of the dipole field in this geometry. This field will set up currents in the cylinder that give rise to the induced field. If $d \gg a$, we may do WKB: use the uniform solution but with an applied field that varies slowly with z. In this approximation the dipole moment per unit length at z is proportional to the applied field at z with the polarizability already given above. Thus

$$\begin{aligned} M_z(z) &= \pi a^2 \alpha_z B(z) \\ &= \pi a^2 \alpha_z m\frac{2z^2-d^2}{(z^2+d^2)^{5/2}} \end{aligned}$$

and this sets up an induced field at $\vec{r}$ which is

$$\begin{aligned} B_z^{(ind)} &= \int_{-\infty}^{\infty} dz\ M_z(z)\frac{2z^2-d^2}{(z^2+d^2)^{5/2}} \\ &= \frac{\pi a^2\alpha_z m}{d^5} I_z, \end{aligned}$$

where

$$I_z = \int_{-\infty}^{\infty} dx \frac{\left(2x^2-1\right)^2}{\left(1+x^2\right)^5} = \frac{27\pi}{128.}.$$

According to the usual prescription, then we find

$$\langle B_z(\vec{r})\, B_z(\vec{r})\rangle = \frac{27\pi\hbar a^2}{256d^5}\,\mathrm{Im}\left[\frac{2}{ka}\frac{J_1(ka)}{J_0(ka)}\right]\coth\left(\frac{\hbar\omega}{2k_BT}\right),$$

valid for any value of δ/a.

When $a \gg \delta$ we expand the Bessel functions for small argument and find

$$\begin{aligned} B_z^{(ind)} &= \frac{\pi a^2\alpha_z m}{d^5}\frac{27\pi}{128} \\ \langle B_z(\vec{r})\, B_z(\vec{r})\rangle &= \frac{27\pi\hbar a^4}{2048 d^5\delta^2}\coth\left(\frac{\hbar\omega}{2k_BT}\right). \end{aligned}$$

The same computation can be performed for the x and y directions. The results for $i = j = x$ are

$$\langle B_x(\vec{r})\, B_x(\vec{r})\rangle = \frac{123\pi\hbar a^2}{256d^5}\,\mathrm{Im}\left[\frac{2}{ka}\frac{J_1(ka)}{J_0(ka)}\right]\coth\left(\frac{\hbar\omega}{2k_BT}\right),$$

valid for any value of δ/a and for $a \gg \delta$ we have

$$\langle B_x(\vec{r})\, B_x(\vec{r})\rangle = \frac{123\pi\hbar a^4}{1024\ d^5\delta^2}\coth\left(\frac{\hbar\omega}{2k_BT}\right),$$

while for $i = j = y$

$$\langle B_y(\vec{r})\, B_y(\vec{r})\rangle = \frac{3\pi\hbar a^2}{32d^5}\,\mathrm{Im}\left[\frac{2}{ka}\frac{J_1(ka)}{J_0(ka)}\right]\coth\left(\frac{\hbar\omega}{2k_BT}\right),$$

valid for any value of δ/a and for $a \gg \delta$

$$B_y^{(ind)} = \frac{\pi a^2 \alpha_y m}{d^5} \frac{3\pi}{16}$$
$$\langle B_y(\vec{r})\, B_y(\vec{r})\rangle = \frac{3\pi\hbar a^4}{128 d^5 \delta^2} \coth\left(\frac{\hbar\omega}{2k_B T}\right).$$

These considerations lead to very subtantial anisotropy in the correlation functions and in the relaxation times. We have that for $d \gg a$

$$\langle B_x(\vec{r})\, B_x(\vec{r})\rangle : \langle B_y(\vec{r})\, B_y(\vec{r})\rangle : \langle B_z(\vec{r}')\, B_z(\vec{r})\rangle = 82 : 16 : 9.$$

5.3. Distant Object

We now treat the magnetic noise of a metallic object whose maximum linear dimension is short compared with the distance to the qubit: $d \gg L$. We consider a fictitious point magnetic dipole $\vec{m}$ at $\vec{r}'$ and a magnetically polarizable metallic object at the origin. The observation point is $\vec{r}$. Since L is small, we may take the field $\vec{B}'$ at the object due to the test dipole to be uniform over the object. If we assume that the electrode is spherical and its dielectric function is isotropic then the magnetic polarizability can be written as $\beta_{jn}(\omega) = \delta_{jn}\beta(\omega)$ and Eq. (29) gives the physical correlation function:

$$\langle B_i(\vec{r})\, B_k(\vec{r}')\rangle = \hbar \coth\left(\frac{\hbar\omega}{2k_B T}\right) \mathrm{Im}\,\beta \frac{3x'_j x'_k - \delta_{jk} r'^2}{r'^5} \frac{3x_i x_j - \delta_{ij} r^2}{r^5}$$

This manifestly satisfies the Onsager relation

$$G_{ik}(\omega; \vec{r}, \vec{r}') = G_{ki}(\omega; \vec{r}', \vec{r}).$$

The local noise at $\vec{r} = \vec{r}'$ is

$$\langle B_i(\vec{r})\, B_k(\vec{r}' = \vec{r})\rangle = \hbar \coth\left(\frac{\hbar\omega}{2k_B T}\right) \mathrm{Im}(\beta) \frac{3x_i x_k + \delta_{ik} r^2}{r^8}. \tag{52}$$

The r^{-6} dependence is familiar from the van der Waals force, which has a similar physical origin.

Thus the problem reduces to a calculation of $\mathrm{Im}[\beta(\omega)]$, the dissipative part of the polarizability of the electrode. For a spherical electrode with radius a and conductivity σ, we have that [35]

$$\mathrm{Im}\,\beta = -\frac{3\delta^2 a}{4}\left[1 - \frac{a\sinh(2a/\delta) + \sin(2a/\delta)}{\cosh(2a/\delta) - \cos(2a/\delta)}\right],$$

which reduces when $\delta \gg a$ to

$$\mathrm{Im}\,\beta = \frac{a^5}{15\delta^2}$$

and when $\delta \ll a$ to

$$\mathrm{Im}\,\beta = \frac{3a^2\delta}{4}.$$

Notice that the *anisotropy* in lifetimes of a qubit in the presence of a spherical electrode is independent of β. If the qubit is located at $\vec{r} = r\hat{z}$, then

$$\langle B_x(\vec{r})\, B_x(\vec{r}' = \vec{r})\rangle = \langle B_y(\vec{r})\, B_y(\vec{r}' = \vec{r})\rangle = \hbar \coth\left(\frac{\hbar\omega}{2k_B T}\right) \frac{\mathrm{Im}[\beta(\omega)]}{r^6}$$

$$\langle B_z(\vec{r})\, B_z(\vec{r}' = \vec{r})\rangle = 4\hbar \coth\left(\frac{\hbar\omega}{2k_B T}\right) \frac{\mathrm{Im}[\beta(\omega)]}{r^6}.$$

The anisotropy

$$\langle B_z(\vec{r})\, B_z(\vec{r})\rangle = 4\langle B_x(\vec{r})\, B_x(\vec{r})\rangle$$

is stronger than in the half-space case.

6. NUMERICAL ESTIMATES

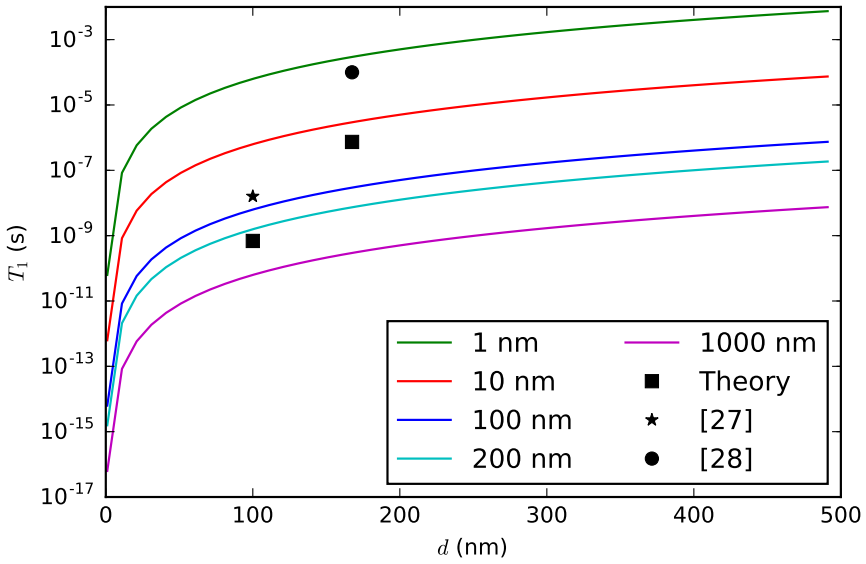

FIG. 7: The charge qubit relaxation time T_1 as a function of the distance d from the qubit to a planar metal gate for various values of the dot separation, as listed in the inset. The experimental data are taken from Ref. [27, 28]. The theoretical predictions are indicated by solid squares. The qubit operating frequency is taken as $\omega = 10^9$ s^{-1}, while the conductivities are roughly estimated as $\sigma = 10^{16}$ s^{-1}. The temperature is $T = 0.1$ K.

In this section we provide some numerical estimates for the noise strength and the resulting qubit relaxation times, which will allow us to evaluate the relevance of EWJN for current experiments. We shall focus on the half-space geometry, since this case is the important one for existing devices; the greatest masses of metal in semicoductor qubit systems are usually in global gates.

6.1. Charge Qubits

The noise spectral energy density is of some interest. Taking $\omega = 10^9/s$, $\sigma = 10^{17}/s$, we get $\delta = c/\sqrt{2\pi\sigma\omega} = 12 \times 10^{-4}$ cm $= 12\ \mu$ and we will only consider the regime $d \ll \delta$. The vacuum wavelength $\lambda = 60$ cm is the longest length in the problem and plays no role in our quasistatic regime. At a distance d from a half space we find and $T = 1$K and $\varepsilon_d = 10$ we have:

$$\langle E_x(d)\, E_x(d)\rangle_\omega \approx \frac{k_B T}{8\pi\sigma d^3} = 9 \times 10^{-22}\, \frac{erg}{cm^3} s.$$

This noise will relax qubits. In Fig. 7 we give numerical estimates for T_1 of a charge qubit in a half-space geometry. The curves are plotted using Eqs. (35) and (43) assuming a point qubit. Each curve represents $T_1(d)$ for various values of the distance d from the half space and the dot separation L, the latter being listed in the inset. We have assumed $\omega = 10^9$ s^{-1}, $\sigma = 10^{16}$ s^{-1}, $T = 0.1$ K. Indicated on the figure are experimental values for T_1 and the predictions our model makes based on estimates of the particular experiment's qubit and surrounding geometry. The measured values are an order of magnitude or two smaller than the predictions made by our model, indicating that EWJN is probably not the dominant mechanism behind qubit relaxation in these experiments. However, the estimates here are made with very limited knowledge of the particular experimental values of d and L, which are normally not very accurately determined. Since $T_1 \propto d^3/L^2$ a factor of 2 could account for an order of magnitude correction. A further serious source of uncertainty is that σ is not measured and generally is poorly known. If σ is too large, the mean free path is the electrons in the metal may become comparable to the gate dimensions, invalidating the local electrodynamics used in this paper. These considerations taken together mean that it is difficult to give a clear evaluation of the role of EWJN in charge qubit experiments. In any case, it seems safe to say that even rather minor improvements in other decoherence mechanisms would make the EWJN mechanism competitive with the others.

6.2. Spin qubits

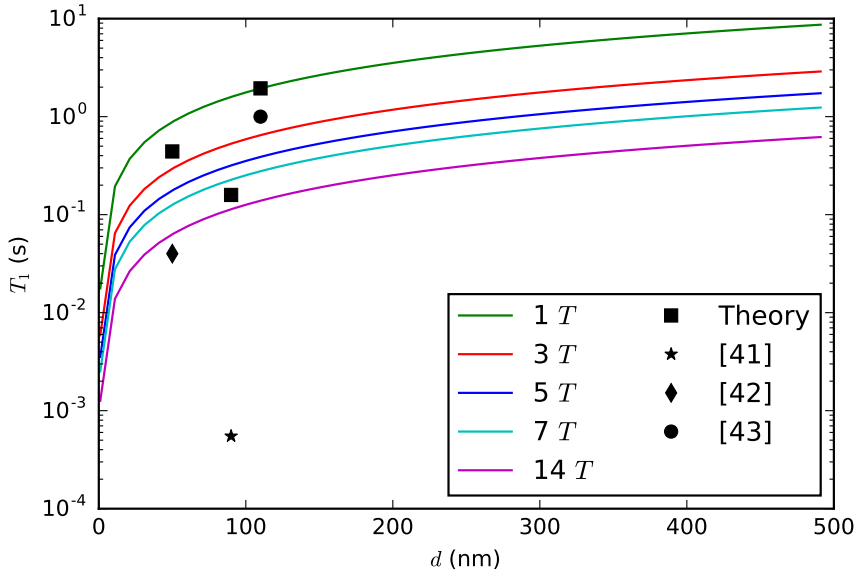

FIG. 8: The spin qubit relaxation time T_1 as a function of the distance d from the qubit to a planar metal gate for various values of the external magnetic field, as listed in the inset. The experimental data are taken from Ref. [39–41]. The theoretical predictions are indicated by solid squares. The conductivities are roughly estimated as $\sigma = 10^{16}$ s^{-1}. The temperature is $T = 0.1$ K.

We can now repeat the numerical estimates for the noise strength and the resulting qubit relaxation times for magnetic noise and spin qubits.

The noise energy density is again of some interest. With $\omega = 10^9/s$, $\sigma = 10^{17}/s$, $T = 1$ K, $d = 50$ nm from a half space we have:

$$\langle B_z B_z \rangle_\omega \approx \frac{\pi k_B T \sigma}{dc^2} = 3.0 \times 10^{-15} \frac{erg\dot{s}}{cm^3}$$

This noise will relax qubits. In Fig. 8 we give numerical estimates for T_1 of a spin qubit in a half-space geometry. The curves are plotted using Eq. (35) assuming a point qubit. Each curve represents $T_1(d)$ for various values of the distance d from the half space for a fixed B field, which enters T_1 via $\hbar\omega = g\mu B$ with $g = 2$. We have assumed $\sigma = 10^{16}$ s^{-1}, $T = 0.1$ K. Indicated on the figure are experimental values for T_1 and the predictions our model makes based on estimates of the particular experiment's qubit and surrounding geometry. The geometries are somewhat better determined in these experiments, meaning that that the main source of uncertainty is in the conductivity σ, which may differ from our assumption by an order of magnitude.

The experimental values shown in Fig. 7 are in small devices characterized by linear dimensions of order 100 nm, but we note that in certain MOS devices the relevant distances can be closer to 10 nm [42, 43]. Other qubit architectures such as atom traps, ion traps, or superconductors, are generally considerably larger. This makes it unlikely that EWJN plays a large role in the decoherence of these devices, since the power-law falloffs reduce the noise strength at the qubit positions. This could change as these devices are miniaturized [44, 45].

7. CONCLUSIONS

Qubits with long relaxation times are necessary for quantum computation. Most such devices are controlled electrically. This creates a control – isolation dilemma: connections from the outside world are what make the devices useful, but they are also sources of decoherence. In particular, one may wish to place charge or spin qubits close to metallic device elements used to confine or control the qubits. However, the fluctuating currents and charges in

metals give rise to noise that leaks out of the metal into the surrounding region, decohereing the qubits. This is standard physics, (though not often treated in textbooks) and results for the noise spectral densities near a half plane are well known. However, results for the more complicated geometries of real devices have not been available at all. The results presented above represent a first step in the direction of repairing this situation.

Most importantly, we have given a streamlined method for the calculation of both noise spectral densities and noise correlation functions. We have presented new results for the spectral density of cylinders and distant objects, and for the noise correlation functions for half spaces and distant objects. The new method also enables us to give more qualitative, but still useful, discussions of issues such as asperities on metal surfaces.

Numerical estimates of the effect of EWJN on qubits indicates that it is proabably not a dominant effect on the current generation of charge qubit devices. For spin qubits the situation is different. Experiments in which the gates are close to the qubits may already be showing the effects of EWJN.

8. ACKNOWLEDGMENTS

We have benefited from discussions with Amrit Poudel, Luke Langsjoen, Andrea Morello, and John Nichol. This work was supported by the ARO under award No. W911NF-12-0607.

[1] J. B. Johnson, "Thermal agitation of electricity in conductors," Phys. Rev. **32**, 97–109 (1928).
[2] H. Nyquist, "Thermal agitation of electric charge in conductors," Phys. Rev. **32**, 110–113 (1928).
[3] Herbert B. Callen and Theodore A. Welton, "Irreversibility and generalized noise," Phys. Rev. **83**, 34–40 (1951).
[4] R. Kubo, "The fluctuation-dissipation theorem," Reports on Progress in Physics **29**, 255 (1966).
[5] E.M. Lifshitz, "The theory of molecular attractive forces between solids," Sov. Phys. JETP **2**, 73 (1956).
[6] S. M. Rytov, *Theory of Electrical Fluctuation and Thermal Radiation* (Publishing House, 1953).
[7] G. S. Agarwal, "Quantum electrodynamics in the presence of dielectrics and conductors. i. electromagnetic-field response functions and black-body fluctuations in finite geometries," Phys. Rev. A **11**, 230–242 (1975).
[8] H. B. G. Casimir, "On the Attraction Between Two Perfectly Conducting Plates," Indag. Math. **10**, 261–263 (1948), [Kon. Ned. Akad. Wetensch. Proc.100N3-4,61(1997)].
[9] E. M. Lifshitz and L.P. Pitaevskii, *Statistical Physics*, Part 2, Vol. 9 (Pergamon, 1980).
[10] A. I. Volokitin and B. N. J. Persson, "Near-field radiative heat transfer and noncontact friction," Rev. Mod. Phys. **79**, 1291–1329 (2007).
[11] J.B. Pendry, "Radiative exchange of heat between nanostructures," J. Phys.: Condensed Matter **11**, 6621–6633 (1999).
[12] R. Neumann and L. R. Schreiber, "Simulation of micro-magnet stray-field dynamics for spin qubit manipulation," Journal of Applied Physics **117**, 193903 (2015), http://dx.doi.org/10.1063/1.4921291.
[13] A. Kha, R. Joynt, and D. Culcer, "Do micromagnets expose spin qubits to charge and johnson noise?" Applied Physics Letters **107**, 172101 (2015), http://dx.doi.org/10.1063/1.4934693.
[14] C. Henkel, S. Pötting, and M. Wilkens, "Loss and heating of particles in small and noisy traps," Applied Physics B **69**, 379–387 (1999).
[15] C. Henkel and M. Wilkens, "Heating of trapped atoms near thermal surfaces," Europhys. Lett. **47**, 414–420 (1999).
[16] D. M. Harber, J. M. McGuirk, J. M. Obrecht, and E. A. Cornell, "Thermally induced losses in ultra-cold atoms magnetically trapped near room-temperature surfaces," Journal of Low Temperature Physics **133**, 229–238 (2003).
[17] J. A. Sidles, J. L. Garbini, W. M. Dougherty, and Shih-Hui Chao, "The classical and quantum theory of thermal magnetic noise, with applications in spintronics and quantum microscopy," Proceedings of the IEEE **91**, 799–816 (2003).
[18] D.V. Averin, "Adiabatic quantum computation with cooper pairs," Solid State Communications **105**, 659 – 664 (1998).
[19] Y. Makhlin, G. Schön, and A. Shnirman, "Quantum-state engineering with josephson-junction devices," Rev. Mod. Phys. **73**, 357–400 (2001).
[20] M. I. Dykman, P. M. Platzman, and P. Seddighrad, "Qubits with electrons on liquid helium," Phys. Rev. B **67**, 155402 (2003).
[21] Peihao Huang and Xuedong Hu, "Electron spin relaxation due to charge noise," Phys. Rev. B **89**, 195302 (2014).
[22] A. Poudel, L. S. Langsjoen, M. G. Vavilov, and R. Joynt, "Relaxation in quantum dots due to evanescent-wave johnson noise," Phys. Rev. B **87**, 045301 (2013).
[23] L. S. Langsjoen, A. Poudel, M. G. Vavilov, and R. Joynt, "Qubit relaxation from evanescent-wave johnson noise," Phys. Rev. A **86**, 010301 (2012).
[24] S. Kolkowitz, A. Safira, A. A. High, R. C. Devlin, S. Choi, Q. P. Unterreithmeier, D. Patterson, A. S. Zibrov, V. E. Manucharyan, H. Park, and M. D. Lukin, "Probing johnson noise and ballistic transport in normal metals with a single-spin qubit," Science **347**, 1129–1132 (2015), http://science.sciencemag.org/content/347/6226/1129.full.pdf.
[25] T. Hayashi, T. Fujisawa, H. D. Cheong, Y. H. Jeong, and Y. Hirayama, "Coherent manipulation of electronic states in a double quantum dot," Phys. Rev. Lett. **91**, 226804 (2003).

[26] T. Fujisawa, T. Hayashi, H.D. Cheong, Y.H. Jeong, and Y. Hirayama, "Rotation and phase-shift operations for a charge qubit in a double quantum dot," Physica E: Low-dimensional Systems and Nanostructures **21**, 1046 – 1052 (2004), proceedings of the Eleventh International Conference on Modulated Semiconductor Structures.
[27] J. R. Petta, A. C. Johnson, C. M. Marcus, M. P. Hanson, and A. C. Gossard, "Manipulation of a single charge in a double quantum dot," Phys. Rev. Lett. **93**, 186802 (2004).
[28] J. Gorman, D. G. Hasko, and D. A. Williams, "Charge-qubit operation of an isolated double quantum dot," Phys. Rev. Lett. **95**, 090502 (2005).
[29] D. C. B. Valente, E. R. Mucciolo, and F. K. Wilhelm, "Decoherence by electromagnetic fluctuations in double-quantum-dot charge qubits," Phys. Rev. B **82**, 125302 (2010).
[30] L. S. Langsjoen, A. Poudel, M. G. Vavilov, and R. Joynt, "Electromagnetic fluctuations near thin metallic films," Phys. Rev. B **89**, 115401 (2014).
[31] R.E. Raab and O.L. De Lange, *Multipole Theory in Electromagnetism* (Oxford Science Publications, 2005).
[32] Jonas Bylander, Simon Gustavsson, Fei Yan, Fumiki Yoshihara, Khalil Harrabi, George Fitch, David G. Cory, Yasunobu Nakamura, Jaw-Shen Tsai, and William D. Oliver, "Noise spectroscopy through dynamical decoupling with a superconducting flux qubit," Nat Phys **7**, 565–570 (2011).
[33] O. E. Dial, M. D. Shulman, S. P. Harvey, H. Bluhm, V. Umansky, and A. Yacoby, "Charge noise spectroscopy using coherent exchange oscillations in a singlet-triplet qubit," Phys. Rev. Lett. **110**, 146804 (2013).
[34] Juha T. Muhonen, Juan P. Dehollain, Arne Laucht, Fay E. Hudson, Rachpon Kalra, Takeharu Sekiguchi, Kohei M. Itoh, David N. Jamieson, Jeffrey C. McCallum, Andrew S. Dzurak, and Andrea Morello, "Storing quantum information for 30 seconds in a nanoelectronic device," Nat Nano **9**, 986–991 (2014), letter.
[35] L.D. Landau and E. M. Lifshitz, *Electrodynamics of Continuous Media*, Vol. 8 (Pergamon, 1980).
[36] J. A. Osborn, "Demagnetizing factors of the general ellipsoid," Phys. Rev. **67**, 351–357 (1945).
[37] A. Garg, "Conductors in quasistatic electric fields," American Journal of Physics **76** (2008).
[38] A. Garg, *Classical Electromagnetism in a Nutshell* (Princeton University Press, 2012).
[39] M. Xiao, M. G. House, and H. W. Jiang, "Measurement of the spin relaxation time of single electrons in a silicon metal-oxide-semiconductor-based quantum dot," Phys. Rev. Lett. **104**, 096801 (2010).
[40] L. H. Willems van Beveren B. Witkamp L. M. K. Vandersypen J. M. Elzerman, R. Hanson and L. P. Kouwenhoven, "Single-shot read-out of an individual electron spin in a quantum dot," Nature **430**, 431–435 (2004).
[41] S. Amasha, K. MacLean, Iuliana P. Radu, D. M. Zumbühl, M. A. Kastner, M. P. Hanson, and A. C. Gossard, "Electrical control of spin relaxation in a quantum dot," Phys. Rev. Lett. **100**, 046803 (2008).
[42] Susan J. Angus, Andrew J. Ferguson, Andrew S. Dzurak, and Robert G. Clark, "Gate-defined quantum dots in intrinsic silicon," Nano Letters **7**, 2051–2055 (2007), pMID: 17567176, http://dx.doi.org/10.1021/nl070949k.
[43] J.C.C. Hwang, C.H. Yang, M. Veldhorst, N. Hendrickx, M.A. Fogarty, W. Huang, F.E. Hudson, A. Morello, and A.S. Dzurak, "Impact of g-factors and valleys on spin qubits in a silicon double quantum dot," ArXiv e-prints (2016), arXiv:1608.07748 [cond-mat.mes-hall].
[44] Ron Folman, Peter Krüger, Donatella Cassettari, Björn Hessmo, Thomas Maier, and Jörg Schmiedmayer, "Controlling cold atoms using nanofabricated surfaces: Atom chips," Phys. Rev. Lett. **84**, 4749–4752 (2000).
[45] M. A. Cirone, A. Negretti, T. Calarco, P. Krüger, and J. Schmiedmayer, "A simple quantum gate with atom chips," The European Physical Journal D - Atomic, Molecular, Optical and Plasma Physics **35**, 165–171 (2005).

Appendix A: Multipole moments in T_1 and T_2

The expressions in Eqs. (35) and (40) can be generalized to higher order multipole moments by keeping more terms in the Taylor expansion of the electromagnetic potentials. Define the electric moments $q_i = er_i$, $q_{ij} = er_ir_j$ and magnetic dipole $m_i = \frac{e}{2mc}((\vec{r}\times\vec{\Pi})_i + gS_i)$. We then have

$$[H_q, p_i] = -\frac{i\hbar e}{m}\Pi_i$$
$$[H_q, q_{ij}] = -\frac{i\hbar q}{m}\left(r_i\Pi_j + r_j\Pi_i - i\hbar\delta_{ij}\right).$$

We can find the quadrupole contribution by expanding Eq. (34) and keeping track of all first derivative terms giving us

$$\begin{aligned}
\langle 0|H_n(t)|1\rangle &= -\frac{e}{mc}\left[A_i(0,t)\,\langle 0|\Pi_i|1\rangle\right. \\
&\quad \left. + \langle 0|\left(\nabla_j A_i(r,t)\right)_{r=0} r_j \Pi_i|1\rangle\right] - \frac{eg}{2mc} B_i\,\langle 0|S_i|1\rangle \\
&= i\frac{\omega}{c}\,\langle 0|p_i|1\rangle\, A_i(0,t) - \frac{e}{mc}\langle 0|\frac{1}{2}[\nabla_j A_i]_{r=0}(r_i\Pi_j + r_j\Pi_i)|1\rangle \\
&\quad - \frac{e}{2mc}(\nabla\times\vec{A})_{k,r=0}\langle 0|\epsilon_{ijk} r_j\Pi_i|1\rangle - \frac{eg}{2mc} B_i\,\langle 0|S_i|1\rangle \\
&= i\frac{\omega}{c}\left(\langle 0|p_i|1\rangle\, A_i(0,t) + \frac{1}{2}[\nabla_j A_i]_{r=0}\,\langle 0|q_{ij}|1\rangle\right) \\
&\quad - B_k(0,t)\,\langle 0|m_k|1\rangle\,.
\end{aligned}$$

We have employed the vector identity

$$\begin{aligned}
[\nabla_j A_i(r,t)]_{r=0}\, r_j\Pi_i &= \frac{1}{2}[\nabla_j A_i]_{r=0}(r_i\Pi_j + r_j\Pi_i) \\
&\quad - \frac{1}{2}\epsilon_{ijk}(\nabla\times\vec{A})_{k,r=0} r_j\Pi_i.
\end{aligned}$$

Now we can work out an expression for T_1 using Eq. (32)

$$\begin{aligned}
\frac{1}{T_1} = \frac{1}{\hbar^2}\Big[&\langle p_i\rangle\,\langle p_l\rangle^*\,\langle E_i E_l\rangle_\omega + \frac{1}{2}\,\langle p_i\rangle\,\langle q_{lm}\rangle^*\,\langle E_i\nabla_m E_l\rangle_\omega + \frac{1}{2}\,\langle q_{ij}\rangle\,\langle p_l\rangle^*\,\langle\nabla_j E_i E_l\rangle_\omega \\
&+ \langle p_i\rangle\,\langle m_n\rangle^*\,\langle E_i B_n\rangle_\omega + \langle m_k\rangle\,\langle p_l\rangle^*\,\langle B_k E_l\rangle_\omega + \langle m_k\rangle\,\langle m_n\rangle^*\,\langle B_k B_n\rangle_\omega \\
&- \frac{1}{2}\,\langle q_{ij}\rangle\,\langle m_n\rangle^*\,\langle\nabla_j E_i B_n\rangle_\omega + \frac{1}{2}\,\langle m_k\rangle\,\langle q_{lm}\rangle^*\,\langle B_k\nabla_m E_l\rangle_\omega + \frac{1}{4}\,\langle q_{ij}\rangle\,\langle q_{lm}\rangle^*\,\langle\nabla_j E_i\nabla_m E_l\rangle\Big]\,.
\end{aligned}$$

A naive application of the analysis from the preceeding calculation would indicate that E-field noise will not contribute to diagonal elements of $H_n(t)$, but this is due to the incomplete application of the gauge condition $\phi = 0$. If we begin with the gauge-invariant Schrö dinger equation with an arbitrary scalar potential $\phi(r,t)$ and vector potential obeying $\nabla\cdot\vec{A} = 0$ and eliminate the residual gauge freedom via $\vec{A}'(r,t) = \vec{A}(r,t) + \nabla\alpha(r,t)$, $\phi'(r,t) = \phi(r,t) - \dot{\alpha}(r,t) = 0$ and $\psi' = e^{-ie\alpha/\hbar}\psi(r,t)$ we find that the wave function obeys

$$i\hbar\dot{\psi} = \left(e^{ie\alpha/\hbar} H' {}^{-ie\alpha/\hbar} - e\dot{\alpha}\right)\psi.$$

The Hamiltonian H' in the gauge with no scalar potential is complemented by the gauge fixing term that retains the electric field contribution in the equations of motion. The operator we need in Eq. (39) can be expanded in Taylor series as

$$\begin{aligned}
H_n(t) &= -\frac{e}{mc}\left(A_i(0,t) + [\nabla_j A_i(r,t)]_{r=0}\, r_j + \dots\right)\Pi_i \\
&\quad - \frac{eg}{2mc} B_i S_i. - e\left(\dot{\alpha}(0,t) + \nabla_j\dot{\alpha}(0,t) r_j + \dots\right). \qquad \text{(A1)}
\end{aligned}$$

Now turning to the relevant matrix elements of Eq. (34) with the gauge term (equivalently, the scalar potential), we begin by treating the vector potential terms

$$\begin{aligned}
-\frac{e}{mc}\,\langle 1|A_i(0,t)\Pi_i|1\rangle &= \frac{i}{\hbar c} A_i(0,t)\left(\langle 1|p_i H_q|1\rangle - \langle 1|H_q p_i|1\rangle\right) \\
&= \frac{i}{\hbar c} A_i(\epsilon_1 - \epsilon_1)\,\langle 1|p_i|1\rangle = 0, \\
-\frac{e}{mc}\,\langle 1|\nabla_j A_i r_j\Pi_i|1\rangle &= -\frac{e}{mc}\left[\frac{1}{2}\nabla_j A_i\,\langle 1|r_i\Pi_j + r_j\Pi_i|1\rangle\right. \\
&\qquad \left. + \frac{1}{2} B_k\,\langle 1|l_k|1\rangle\right] \\
&= -\frac{e}{mc}\left(\frac{i\hbar}{2}\nabla_j A_i\delta_{ij}\right) - \frac{e}{2mc} B_k\,\langle 1|l_k|1\rangle \\
&= -\frac{e}{2mc} B_k\,\langle 1|l_k|1\rangle\,.
\end{aligned}$$

The last equality follows from $\nabla \cdot \vec{A} = 0$. We have $E_i(r,t) = -\nabla_i \dot{\alpha}(r,t)$. Using the same methods we obtain an expression for the integral kernel $S(\omega)$ for T_2 to quadrupole order.

$$\begin{aligned} S(\omega) = \frac{1}{\hbar^2} \Big[& \langle B_i(t) B_j(0) \rangle_\omega \, \Delta m_i \Delta m_j - \langle B_i(t) E_j(0) \rangle_\omega \, \Delta m_i \Delta p_j - \langle E_i(t) B_j(0) \rangle_\omega \, \Delta p_i \Delta m_j \\ & + \langle E_i(t) E_j(0) \rangle_\omega \, \Delta p_i \Delta p_j + \frac{1}{2} \left(\langle \nabla_i E_j(t) B_k(0) \rangle_\omega \, \Delta q_{ij} \Delta m_k + \langle \nabla_i E_j(t) E_k(0) \rangle_\omega \, \Delta q_{ij} \Delta p_k \right. \\ & \left. + \langle B_i(t) \nabla_j E_k(0) \rangle \, \Delta m_i \Delta q_{jk} + \langle E_i(t) \nabla_j E_k(0) \rangle_\omega \, \Delta p_i \Delta q_{jk} \right) \frac{1}{4} \langle \nabla_i E_j(t) \nabla_k E_l(0) \rangle_\omega \, \Delta q_{ij} \Delta q_{kl} \Big] \end{aligned}$$

Appendix B: Spectral Density Tensors

Here we include the details and off-diagonal components of the noise spectral density tensor for the simple geometries treated in the main body of the paper.

1. Electric Noise

Place a fictitious electric dipole moment $\vec{p}$ at the point $\vec{r}' = (0,0,d)$ in the half-space geometry. The electric field in free space would be

$$E_j^{(ed)}(\vec{r}) = -\frac{\partial}{\partial x_j} \vec{p} \cdot \nabla \frac{1}{|\vec{r} - \vec{r}'|} = -p_k \frac{\partial}{\partial x_j} \frac{\partial}{\partial x_k} \frac{1}{|\vec{r} - \vec{r}'|}, \tag{B1}$$

which satisfies $\nabla \cdot \vec{E}^{(ed)} = 4\pi\rho$ with $\rho = -\vec{p} \cdot \nabla \delta^3(\vec{r} - \vec{r}_0)$.

We will represent this fictitious field by using the identity

$$\frac{1}{|\vec{r} - \vec{r}'|} = \frac{1}{2\pi} \int \frac{d^2q}{q} \; e^{i\vec{q}\cdot\vec{\rho}} e^{-q|z-d|},$$

where $\vec{q} = (q_x, q_y)$ and $\vec{\rho} = (x,y)$. Thus

$$E_j^{(ed)}(\vec{r}) = -\frac{p_k}{2\pi} \int \frac{d^2q}{q} \frac{\partial}{\partial x_j} \frac{\partial}{\partial x_k} \; e^{i\vec{q}\cdot\vec{\rho}} e^{-q|z-d|}.$$

The induced field for $z > 0$ is expanded as

$$E_j^{(ind)}(\vec{r}) = -\frac{p}{2\pi} \int d^2q \; f_j(\vec{q}) \, e^{i\vec{q}\cdot\vec{\rho}} e^{-qz},$$

and the Maxwell equations imply

$$\nabla^2 \vec{E}^{(ind)} = 0, \; \nabla \cdot \vec{E}^{(ind)} = 0, \; z > 0,$$

so

$$\begin{aligned} q &= \sqrt{q_x^2 + q_y^2} \\ iq_x f_x + iq_y f_y &= q f_z. \end{aligned}$$

The induced field for $z < 0$ is defined by

$$E_j^{(ind)}(\vec{r}) = -\frac{p}{2\pi} \int d^2q \; g_j(\vec{q}) \, e^{i\vec{q}\cdot\vec{\rho}} e^{\alpha z}$$

and we have

$$\nabla^2 \vec{E}^{(ind)} + 2i\delta^{-2}\vec{E}^{(ind)} = 0,\ \nabla \cdot \vec{E}^{(ind)} = 0,\ z < 0$$

and $\mathrm{Re}\,\alpha > 0$ and so

$$\alpha^2 = q_x^2 + q_y^2 - 2i\delta^{-2} = q^2 - 2i\delta^{-2}$$
$$iq_x g_x + iq_y g_y = -\alpha g_z.$$

The tangential component of $\vec{E}$ is continuous but the normal component satisfies $\vec{E}_{norm,out} = \varepsilon \vec{E}_{norm,in} \approx (4\pi i\sigma/\omega)\,\vec{E}_{norm,in}$, so $\left|\vec{E}_{norm,out}\right| \gg \left|\vec{E}_{norm,in}\right|$. $\vec{B}$ is continuous. The fictitious dipole $\vec{p} = p\hat{z}$ produces a field for $0 < z < d$

$$E_x^{(ed)}(\vec{r}) = -\frac{p}{2\pi}\int d^2q\ iq_x\ e^{i\vec{q}\cdot\vec{\rho}} e^{q(z-d)}$$
$$E_y^{(ed)}(\vec{r}) = -\frac{p}{2\pi}\int d^2q\ iq_y\ e^{i\vec{q}\cdot\vec{\rho}} e^{q(z-d)}$$
$$E_z^{(ed)}(\vec{r}) = -\frac{p}{2\pi}\int d^2q\ q\ e^{i\vec{q}\cdot\vec{\rho}} e^{q(z-d)},$$

and the induced field is defined by

$$\vec{E}^{(ind)} = -\frac{p}{2\pi}\int d^2q\ \vec{f}(\vec{q})\, e^{i\vec{q}\cdot\vec{\rho} - qz} \text{ for } z > 0 \text{ and}$$
$$\vec{E}^{(ind)} = -\frac{p}{2\pi}\int d^2q\ \vec{g}(\vec{q})\, e^{i\vec{q}\cdot\vec{\rho} + \alpha z} \text{ for } z < 0.$$

The boundary conditions yield

$$iq_x e^{-qd} + f_x = g_x$$
$$iq_y e^{-qd} + f_y = g_y$$
$$qe^{-qd} + f_z = (\varepsilon_m/\varepsilon_d)\, g_z$$
$$iq_x f_x + iq_y f_y = q f_z$$
$$iq_x g_x + iq_y g_y = -\alpha g_z.$$

The solution is

$$(f_x, f_y, f_z) = (-iq_x, -iq_y, q)\, e^{-qd}\frac{1 - (\varepsilon_m/\varepsilon_d)\, q/\alpha}{1 + (\varepsilon_m/\varepsilon_d)\, q/\alpha},$$

which gives us an integral expression for the induced field and thus 46. For $\vec{p} = p\hat{x}$ the dipole produces a field for $0 < z < d$

$$E_x^{(ed)}(\vec{r}) = \frac{p}{2\pi}\int \frac{d^2q\ q_x^2}{q}\ e^{i\vec{q}\cdot\vec{\rho}} e^{q(z-d)}$$
$$E_y^{(ed)}(\vec{r}) = \frac{p}{2\pi}\int \frac{d^2q\ q_x q_y}{q}\ e^{i\vec{q}\cdot\vec{\rho}} e^{q(z-d)}$$
$$E_z^{(ed)}(\vec{r}) = -\frac{ip}{2\pi}\int \frac{d^2q\ q_x q}{q}\ e^{i\vec{q}\cdot\vec{\rho}} e^{q(z-d)}.$$

For $d \ll \delta$ we find

$$\begin{aligned}
\mathrm{Im}\,\vec{E}^{(ind)}(\vec{r}) &= -\frac{p}{2\pi}\frac{\omega\varepsilon_d}{2\pi\sigma}\frac{\partial}{\partial x}\nabla\int d^2q\ \frac{1}{q} e^{-q(d+z)} e^{iq_x x + iq_y y} \\
&= -\frac{p}{2\pi}\frac{\omega\varepsilon_d}{\sigma}\frac{\partial}{\partial x}\nabla\frac{1}{\left[(z+d)^2 + \rho^2\right]^{1/2}} \\
&= \frac{p}{2\pi}\frac{\omega\varepsilon_d}{\sigma}\nabla\frac{x}{\left[(z+d)^2 + \rho^2\right]^{3/2}}.
\end{aligned}$$

So, for example,

$$\mathrm{Im}\, E_x^{(ind)}\left(\vec{r}\right) = -\frac{p}{2\pi}\frac{\omega\varepsilon_d}{\sigma}\frac{2x^2-(z+d)^2-y^2}{\left[(z+d)^2+\rho^2\right]^{5/2}}.$$

In the regime $d \gg \delta$ we find

$$\begin{aligned}\mathrm{Im}\,\vec{E}^{(ind)}\left(\vec{r}\right) &= -\frac{p}{2\pi}\frac{\omega\varepsilon_d}{2\pi\sigma\delta}\frac{\partial}{\partial x}\nabla\int d^2q\ \frac{1}{q^2}e^{-q(d+z)}e^{iq_x x+iq_y y}\\ &= \frac{p}{2\pi}\frac{\omega\varepsilon_d}{\sigma\delta}\nabla\left\{\frac{x}{\rho^2}\left[1-\frac{d+z}{\left[(z+d)^2+\rho^2\right]^{1/2}}\right]\right\},\end{aligned}$$

which gives us the correlation functions presented in the main text.

For $\vec{p}=p\hat{z}$ and $d \ll \delta$ the off-diagonal components are:

$$\left\langle E_x\left(\vec{r}=(\vec{\rho},z)\right)E_z\left(\vec{r}'=(0,0,d)\right)\right\rangle_\omega = \frac{3\hbar\omega\varepsilon_d}{2\pi\sigma}\frac{x\left(d+z\right)}{\left[(d+z)^2+\rho^2\right]^{5/2}}\coth\frac{\hbar\omega}{2k_BT}, \tag{B2}$$

$$\left\langle E_y\left(\vec{r}=(\vec{\rho},z)\right)E_z\left(\vec{r}'=(0,0,d)\right)\right\rangle_\omega = \frac{3\hbar\omega\varepsilon_d}{2\pi\sigma}\frac{y\left(d+z\right)}{\left[(d+z)^2+\rho^2\right]^{5/2}}\coth\frac{\hbar\omega}{2k_BT}.$$

When $d \gg \delta$ we have

$$\left\langle E_x\left(\vec{r}=(\vec{\rho},z)\right)E_z\left(\vec{r}'=(0,0,d)\right)\right\rangle_\omega = \frac{\hbar\omega\varepsilon_d}{2\pi\sigma\delta}\frac{x}{\left[(d+z)^2+\rho^2\right]^{3/2}}\coth\frac{\hbar\omega}{2k_BT}, \tag{B3}$$

$$\left\langle E_y\left(\vec{r}=(\vec{\rho},z)\right)E_z\left(\vec{r}'=(0,0,d)\right)\right\rangle_\omega = \frac{\hbar\omega\varepsilon_d}{2\pi\sigma\delta}\frac{y}{\left[(d+z)^2+\rho^2\right]^{3/2}}\coth\frac{\hbar\omega}{2k_BT}.$$

Now we turn to the solution for $\vec{p}=p\hat{x}$ and $d \ll \delta$. The off-diagonal components are

$$\left\langle E_y\left(\vec{r}\right)E_x\left(\vec{r}=\vec{r}'\right)\right\rangle_\omega = \frac{3\hbar\omega\varepsilon_d}{2\pi\sigma}\frac{xy}{\left[(z+d)^2+\rho^2\right]^{5/2}}\coth\frac{\hbar\omega}{2k_BT} \tag{B4}$$

$$\left\langle E_z\left(\vec{r}\right)E_x\left(\vec{r}=\vec{r}'\right)\right\rangle_\omega = -\frac{3\hbar\omega\varepsilon_d}{2\pi\sigma}\frac{x\left(d+z\right)}{\left[(z+d)^2+\rho^2\right]^{5/2}}\coth\frac{\hbar\omega}{2k_BT},$$

and comparison with Eq. (B2) shows that the Onsager relation is satisfied.

The off-diagonal components when $d \gg \delta$ are:

$$\begin{aligned}\left\langle E_y\left(\vec{r}\right)E_x\left(\vec{r}'\right)\right\rangle_\omega = &-\frac{\hbar}{2\pi}\frac{\omega\varepsilon_d}{\sigma\delta}\coth\frac{\hbar\omega}{2k_BT}\times\\ &\frac{xy}{\rho^2}\left\{\frac{2}{\rho^2}\left[1-\frac{d+z}{\left[(z+d)^2+\rho^2\right]^{1/2}}\right]-\frac{d+z}{\left[(z+d)^2+\rho^2\right]^{3/2}}\right\}.\end{aligned} \tag{B5}$$

$$\left\langle E_z\left(\vec{r}\right)E_x\left(\vec{r}'\right)\right\rangle_\omega = -\frac{\hbar}{2\pi}\frac{\omega\varepsilon_d}{\sigma\delta}\frac{x}{\left[(z+d)^2+\rho^2\right]^{3/2}}\coth\frac{\hbar\omega}{2k_BT},$$

and comparison with Eq. (B3) shows that the Onsager relation is satisfied.

For the distant object geometry Since L, the qubit size, is small, we may take the field $\vec{E}'$ at the electrode due to the test dipole to be uniform over the object. It is given by

$$\begin{aligned} E'_j(\vec{r}=0) &= p_k\ \partial_j\partial_k \frac{1}{|\vec{r}'|} \\ &= p_k \frac{3x'_j x'_k - \delta_{jk} r'^2}{r'^5} = p_k f_{jk}(\vec{r}), \end{aligned}$$

where we have defined the dipole function

$$f_{ij}(\vec{r}) \equiv \frac{3x_i x_j - \delta_{ij} r^2}{r^5}.$$

We shall take only the first term in the multipole expansion of the field produced by the object. We will write this dipole as $\vec{p}^{(el)}$ ("el" for "electrode".) It can be written as $p_j^{(el)}(\omega) = \alpha_{jn}(\omega) E'_n(\omega)$. At the observation point $\vec{r}$ the (again fictitious) field is

$$\begin{aligned} E_i(\vec{r}) &= p_j^{(el)} \partial_i \partial_j \frac{1}{|\vec{r}|} \\ &= \alpha_{jn} E'_n f_{ij}(\vec{r}) \\ &= \alpha_{jn} p'_m f_{mn}(\vec{r}')\, f_{ij}(\vec{r}), \end{aligned}$$

This leads directly to

$$\langle E_i(\vec{r})\, E_k(\vec{r}')\rangle = \hbar \coth\left(\frac{\hbar\omega}{2k_B T}\right) \mathrm{Im}(\alpha_{jn})\, f_{kn}(\vec{r}')\, f_{ij}(\vec{r}). \tag{B6}$$

Hence only the polarizability of the object is relevant in the problem. If we assume that the electrode is spherical and its dielectric function is isotropic then $p_j^{(sph)}(\omega) = \alpha(\omega)\,\delta_{jn} E'_n(\omega)$ and

$$\begin{aligned} E_i^{(sp)}(\vec{r}) &= \alpha(\omega)\, p'_k f_{jk}(\vec{r}') f_{ij}(\vec{r}) \\ &= \alpha(\omega)\, p'_k \frac{9x_i x'_k\ \vec{r}\cdot\vec{r}' + \delta_{ik} r^2 r'^2 - 3x_i x_k r'^2 - 3x'_i x'_k r^2}{r^5 r'^5}. \end{aligned}$$

Using Eq. (22), we have

$$-\frac{\omega^2}{\hbar c^2} G_{ik}(\omega;\vec{r},\vec{r}') = \alpha(\omega)\, f_{ij}(\vec{r})\, f_{jk}(\vec{r}').$$

This manifestly satisfies the Onsager relation

$$G_{ik}(\omega;\vec{r},\vec{r}') = G_{ki}(\omega;\vec{r}',\vec{r}).$$

And we find

$$\langle E_i(\vec{r})\, E_k(\vec{r}')\rangle = \hbar \coth\left(\frac{\hbar\omega}{2k_B T}\right) \mathrm{Im}[\alpha(\omega)]\, f_{kj}(\vec{r}')\, f_{ij}(\vec{r}).$$

2. Magnetic Noise

To find the noise tensor in the half space we place a magnetic dipole moment $\vec{m} = m\hat{z}$ at $\vec{r} = (d,0,0)$ in analogy to the electric field noise calculation. The magnetic field due to this fictitious dipole in free space would be

$$B_j^{(md)}(\vec{r}) = m_i \frac{\partial}{\partial x_i} \frac{\partial}{\partial x_j} \frac{1}{|\vec{r}-\vec{r}'|},$$

which satisfies $\nabla \times \vec{B}^{(md)} = 4\pi\vec{J}/c$ and $\vec{J} = \vec{m} \times \nabla\delta^3\left(\vec{r} - \vec{r}'\right)$. Proceeding analogously to Eq. (B1), we have

$$B_j^{(md)}\left(\vec{r}\right) = \frac{m_k}{2\pi}\int \frac{d^2q}{q}\frac{\partial}{\partial x_j}\frac{\partial}{\partial x_k}\; e^{i\vec{q}\cdot\vec{\rho}}e^{-q|z-d|}.$$

where $\vec{q} = (q_x, q_y)$ and $\vec{\rho} = (x, y)$, and

$$\vec{B}^{(ind)}\left(\vec{r}\right) = -\frac{m}{2\pi}\int d^2q\;\left(-iq_x, -iq_y, q\right)e^{-qd}\frac{1-q/\alpha}{1+q/\alpha}e^{iq_x x + iq_y y - qz}\quad \text{for } z > 0.$$

For $d \ll \delta$ we find

$$\begin{aligned}\frac{1-q/\alpha}{1+q/\alpha} &= \frac{\sqrt{q^2 - 2i\delta^{-2}} - q}{\sqrt{q^2 - 2i\delta^{-2}} + q}\\ &\approx \left(-\frac{i}{2q^2\delta^2}\right)\end{aligned}$$

and

$$\vec{B}^{(ind)}\left(\vec{r}\right) = \frac{im}{4\pi\delta^2}\int d^2q\frac{1}{q^2}\;\left(-iq_x, -iq_y, q\right)e^{-q(z+d)}e^{iq_x x + iq_y y}\quad \text{for } z > 0$$

For $\vec{m} = m\hat{z}$ and $d \ll \delta$ the off-diagonal components of the noise tensor in the half space are:

$$\left\langle B_x\left(\vec{r}\right)B_z\left(\vec{r}'\right)\right\rangle_\omega = \frac{\hbar}{2\delta^2}\frac{x}{\rho^2}\left\{1 - \frac{(d+z)}{\left[(d+z)^2 + \rho^2\right]^{1/2}}\right\}\coth\frac{\hbar\omega}{2k_BT} \tag{B7}$$

$$\left\langle B_y\left(\vec{r}\right)B_z\left(\vec{r}'\right)\right\rangle_\omega = \frac{\hbar}{2\delta^2}\frac{y}{\rho^2}\left\{1 - \frac{(d+z)}{\left[(d+z)^2 + \rho^2\right]^{1/2}}\right\}\coth\frac{\hbar\omega}{2k_BT}.$$

In the regime where $d \gg \delta$ we have

$$\left\langle B_x\left(\vec{r}\right)B_z\left(\vec{r}'\right)\right\rangle_\omega = -\hbar\delta\coth\frac{\hbar\omega}{2k_BT}\times\left[\frac{-12x\left(z+d\right)^2 + 3x\rho^2}{\left[(d+z)^2 + \rho^2\right]^{7/2}}\right] \tag{B8}$$

$$\left\langle B_y\left(\vec{r}\right)B_z\left(\vec{r}'\right)\right\rangle_\omega = -\hbar\delta\coth\frac{\hbar\omega}{2k_BT}\times\left[\frac{-12y\left(z+d\right)^2 + 3y\rho^2}{\left[(d+z)^2 + \rho^2\right]^{7/2}}\right].$$

Now we turn to $\vec{m} = m\hat{x}$ and $d \ll \delta$ where the off-diagonal components are

$$\begin{aligned}\left\langle B_y\left(\vec{r}\right)B_x\left(\vec{r}'\right)\right\rangle_\omega &= \frac{\hbar}{2\delta^2}\coth\frac{\hbar\omega}{2k_BT}\frac{\partial}{\partial x}\left[\frac{y}{\rho}\int_0^\infty dq\;\frac{1}{q}e^{-q(z+d)}J_1\left(q\rho\right)\right] \qquad \text{(B9)}\\ &= \frac{\hbar}{2\pi}\coth\frac{\hbar\omega}{2k_BT}\frac{\partial}{\partial x}\left[\frac{y}{\rho^2}\left\{\left[(d+z)^2 + \rho^2\right]^{1/2} - (d+z)\right\}\right]\\ &= -\frac{\hbar}{4\pi\delta^2}\coth\frac{\hbar\omega}{2k_BT}\left[\frac{-2xy}{\rho^4}\left\{\left[(d+z)^2 + \rho^2\right]^{1/2} - (d+z)\right\} + \frac{xy}{\rho^2}\left[(d+z)^2 + \rho^2\right]^{-1/2}\right]\end{aligned}$$

$$\begin{aligned}\left\langle B_z\left(\vec{r}\right)B_x\left(\vec{r}'\right)\right\rangle_\omega &= -\frac{\hbar}{2\delta^2}\coth\frac{\hbar\omega}{2k_BT}\frac{\partial}{\partial x}\frac{\partial}{\partial z}\int_0^\infty dq\;\frac{1}{q^2}e^{-q(z+d)}J_0\left(q\rho\right) \qquad \text{(B10)}\\ &= \frac{\hbar}{2\delta^2}\coth\frac{\hbar\omega}{2k_BT}\frac{\partial}{\partial x}\int_0^\infty dq\;\frac{1}{q}e^{-q(z+d)}J_0\left(q\rho\right)\\ &= -\frac{\hbar}{2\delta^2}\coth\frac{\hbar\omega}{2k_BT}\frac{x}{\rho^2}\left\{\left[(d+z)^2 + \rho^2\right]^{1/2} - (d+z)\right\}.\end{aligned}$$

On the other hand when $d \gg \delta$ we find

$$\langle B_y(\vec{r})\, B_x(\vec{r}')\rangle_\omega = -15\hbar\delta \coth\frac{\hbar\omega}{2k_BT}\frac{xy(d+z)}{\left[(d+z)^2+\rho^2\right]^{7/2}} \tag{B11}$$

$$\langle B_z(\vec{r})\, B_x(\vec{r}')\rangle_\omega = \hbar\delta \coth\frac{\hbar\omega}{2k_BT}\frac{-12x(d+z)^2+3x\rho^2}{\left[(d+z)^2+\rho^2\right]^{7/2}}. \tag{B12}$$

The distant object geometry results can be obtained by placing a fictitious dipole near a magnetically polarizable electrode. Since $d \gg L$ we assume the field generated by this electrode is uniform over the qubit and given by

$$B'_k(0) = m_j\ f_{kj}(\vec{r}'),$$

where again $f_{jk}(\vec{r}) = \left(3r_ir_j - r^2\delta_{ij}\right)/r^5$. We shall take only the first term in the multipole expansion of the field produced by the object, which is completely characterized by its dipole moment $\vec{m}'$. Assuming linear response yields $m'_i = \beta_{ij}B'_j$, where β_{ij} is the magnetic polarizability of the object. At the observation point $\vec{r}$ the (again fictitious) field is

$$\begin{aligned} B_i(\vec{r}) &= m'_m f_{im}(\vec{r}) \\ &= \beta_{mk}m_j\ f_{kj}(\vec{r}')\, f_{im}(\vec{r}), \end{aligned}$$

and the prescription following Eq. 28 then gives the physical noise function as

$$\langle B_i(\vec{r})\, B_j(\vec{r}')\rangle = \hbar\,\mathrm{Im}(\beta_{mk})\ f_{kj}(\vec{r}')\, f_{im}(\vec{r})\coth(\hbar\omega/k_BT).$$

This leads directly to

$$\langle B_i(\vec{r})\, B_k(\vec{r}')\rangle = \hbar\coth\left(\frac{\hbar\omega}{2k_BT}\right)\mathrm{Im}(\beta_{jn})\, f_{kn}(\vec{r}')\, f_{ij}(\vec{r}). \tag{B13}$$

.